Chemical imaging analysis of the brain with X-ray methods

Joanna F Collingwood, Freddy Adams

PII: S0584-8547(16)30342-1
DOI: doi: 10.1016/j.sab.2017.02.013
Reference: SAB 5210

To appear in: *Spectrochimica Acta Part B: Atomic Spectroscopy*

Received date: 9 November 2016
Revised date: 15 February 2017
Accepted date: 15 February 2017

Please cite this article as: Joanna F Collingwood, Freddy Adams , Chemical imaging analysis of the brain with X-ray methods. The address for the corresponding author was captured as affiliation for all authors. Please check if appropriate. Sab(2017), doi: 10.1016/j.sab.2017.02.013

Title: Chemical imaging analysis of the brain with X-ray methods

Authors: Joanna F Collingwood[1] and Freddy Adams[2]
Institutions: 1. School of Engineering, University of Warwick, UK
2. University of Antwerp, Belgium

Corresponding author contact details: Joanna Collingwood, J.F.Collingwood@warwick.ac.uk
School of Engineering, University of Warwick, Library Road, Coventry, CV4 7AL, UK

Abstract

Cells employ various metal and metalloid ions to augment the structure and the function of proteins and to assist with vital biological processes. In the brain they mediate biochemical processes, and disrupted metabolism of metals may be a contributing factor in neurodegenerative disorders. In this tutorial review we will discuss the particular role of X-ray methods for elemental imaging analysis of accumulated metal species and metal-containing compounds in biological materials, in the context of post-mortem brain tissue. X-rays have the advantage that they have a short wavelength and can penetrate through a thick biological sample. Many of the X-ray microscopy techniques that provide the greatest sensitivity and specificity for trace metal concentrations in biological materials are emerging at synchrotron X-ray facilities. Here, the extremely high flux available across a wide range of soft and hard X-rays, combined with state-of-the-art focussing techniques and ultra-sensitive detectors, makes it viable to undertake direct imaging of a number of elements in brain tissue. The different methods for synchrotron imaging of metals in brain tissues at regional, cellular, and sub-cellular spatial resolution are discussed. Methods covered include X-ray fluorescence for elemental imaging, X-ray absorption spectrometry for speciation imaging, X-ray diffraction for structural imaging, phase contrast for enhanced contrast imaging and scanning transmission X-ray microscopy for spectromicroscopy. Two- and three-dimensional (confocal and tomographic) imaging methods are considered as well as the correlation of X-ray microscopy with other imaging tools.

Keywords: synchrotron; metallomics; microscopy; spectroscopy; neurodegeneration

Graphical Abstract

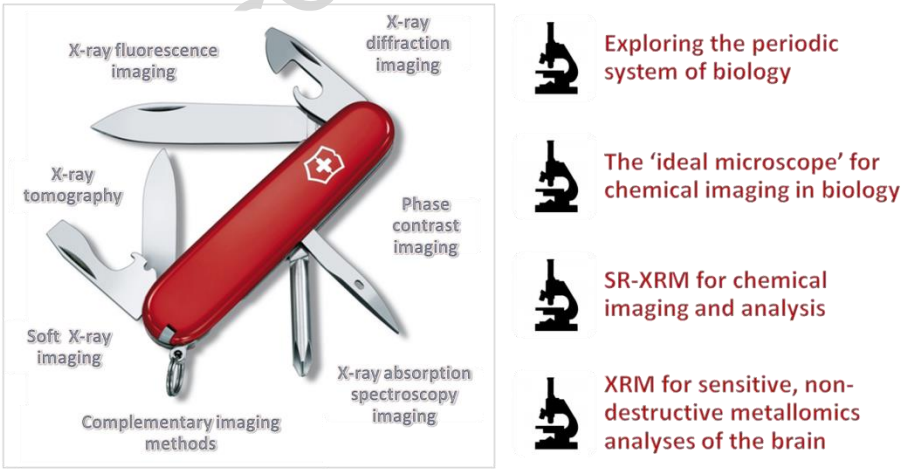

Highlights:

- Motivation for the visualization of metals in tissues of the brain is explored.
- Elements are considered in the context of a Periodic System of Elements in biology.
- Established and emerging X-ray imaging and spectroscopy methods are surveyed.
- The practical aspects of chemical imaging in brain tissues are considered.

1. Introduction

Living systems depend on their ability to accumulate, release and use certain metals. With their rich coordination chemistry and redox properties, cells employ a host of biologically essential metal ions to augment protein structure and function and to carry out vital life processes. The spatial distributions of specific metals and their compounds are as important as their chemical properties, because both their localization and their concentration change in biological systems, and their transport and compartmentalization is critical for effective utilization. In the human body, the central nervous system has an immense biological complexity as a command center for cognitive and motor functions [1]. The role that may be played by the gut in regulating central nervous system behavior is a burgeoning area of enquiry [2]. The brain contains numerous endogenous compounds that are involved in signaling, biosynthesis, and metabolic processes. Metals are particularly important during specific neurological events and in many neurodegenerative diseases.

Metal homeostasis is defined as the metal uptake, trafficking, efflux, and sensing pathways that allows organisms to maintain an appropriate (often narrow) intracellular concentration range of essential metals [3]. Metal homeostasis must be maintained by coordinated uptake, tracking and efflux pathways that place the required amount of the required metal at the required place and time in the cell [4]. The inventory of metals and their species in cells and tissues (including metalloproteins and/or metalloenzymes) is termed as the **metallome** and the analysis thereof as **metallomics** [5]. Imaging and quantifying sub-cellular structures provides essential information about cell function, especially if this is done non-destructively without altering the cellular structure [6]. In general, sample preparation methods for chemical imaging analysis should maintain the localization of the analytes of interest without causing any degradation. Since cells and tissue sections are more or less transparent for high–energy X–rays, this allows the investigation of the interior of thick biological samples, without destructive sample preparation, using three dimensional imaging methods [7].

It was the need to ‘see inside’ opaque objects, especially biological tissues, and to resolve features too small for optical microscopes, or too thick for electron microscopes, that spurred the development of X-ray microscopes to create images with higher resolution than visible or UV light, their wavelength being less than a tenth of a nanometer for energetic X-rays above an energy of 10 keV. This much shorter wavelength means they are less hindered by the diffraction limit which has historically limited spatial observation to micro dimensions for visible or UV light, a disadvantage that could only recently be addressed with super-resolution microscopy techniques [8]. It is possible to use X-rays to visualize cells without the need for chemical fixation, dehydration, or staining of the specimen. As such, X-ray methods are better suited than routine light and electron-based methods (excepting where stabilization with cryo-techniques is possible [9]) for imaging native-state specimens at the functionally important spatial resolution of a few tens of nanometers [6], minimizing interventions which will alter the metal chemistry in the sample such as changes in metal oxidation states. For intracellular imaging of metal species in delicate biological samples such as brain tissues, it is now possible, using the intense X-ray beams of synchrotron X-ray facilities, to achieve

nanometer spatial resolution with sub-ppm detection limits for the wide range of metallic elements that may be present in the normal or malfunctioning brain.

The rationale for investigating metals in the brain is multi-fold. The excellent sensitivity and specificity achievable with X-ray microscopy (XRM) allows the investigation of metal toxicity, for example from environmental exposure to heavy metals such as cadmium, mercury, and arsenic [10-12]. It also supports studies of the normally functioning brain and investigation of disease-mediated changes to the storage and metabolism of biologically-essential metal elements which may occur in specific intracellular compartments [13], or as widespread accumulation in multiple regions of the brain [14]. It continues to grow in utility for the evaluation of brain tissues during the development of metal-containing compounds and tracers for treatment, clinical imaging and improved diagnostic techniques as reviewed elsewhere [15, 16]. With the emergence of new technologies, imaging the distribution of metal species and compounds in animal models of disease in pre-clinical studies is an important tool to evaluate the impact of interventions before they are attempted in clinical trials.

2. The Periodic System of Elements in Biology

According to Maret, 21 elements are presently defined as essential for human life, with a number of additional elements known to be beneficial but not yet confirmed as essential [17]. This list includes a controversial one, chromium that in its trivalent valence state is essential and in the hexavalent state toxic. Other elements are essential in some particular species or in particular ecological niches.

The main category of elemental constituents of biological materials are those involved in synthetic **organic chemistry;** hydrogen, carbon, nitrogen, oxygen, chlorine and sulfur show much cellular ultrastructure and are, up to oxygen, difficult to detect in absorption contrast or fluorescence with multi-keV X-rays. They have low fluorescence yields and little absorption contrast. These components are more easily studied with soft X-rays, see section 4.9. Soft X-ray imaging that utilizes the energy spectra from these elements can provide contextual information about the local environment that complements imaging of other metals (by permitting detailed imaging of tissue structure, and identification of signatures specific to certain proteins, for example).

Alkali and earth alkaline metals such as sodium, potassium, magnesium, and calcium ions are present in *ca* 0.1 molar concentration in tissues and have been studied over a long time in neurobiology [1]. In kinetically labile form, reversibly binding cellular targets, they are involved in active cell transport or cell signaling processes [4]. These elements are not a focus for this review. The comparatively high concentration of these metals in the brain has long-enabled optical imaging, particularly in conjunction with fluorescent probes and indicators [1]. Although synchrotron radiation techniques offer complementary means to investigate structural and temporal aspects of these metals in the brain, optical microscopy continues to underpin many advancements of the field [18, 19].

Phosphorus is essential as a structural component of cell membranes and nucleic acids and involved in many biological processes. **Bromine** was added comparatively recently as an essential element for tissue development and architecture [20]. The main role of **iodine** is as a constituent of thyroid hormones required for brain development. **Sulfur and selenium** are present in amino acids and play characteristic functions in cells. Because of the versatility of sulfur with its many oxidation states and its prevalence in the environment, sulfur evolved to fill many structural, catalytic, and regulatory roles in biology. The experimental and methodological challenge of sulfur speciation in tissues has been addressed with microfocus X-ray absorption spectroscopy (XAS) in the context of brain tumors [21]. In particular, sulfane sulfur, which is sulfur in the thiosulfoxide, has been found to have

regulatory functions in biological systems. The review of Toohey and Cooper outlines the functions of sulfane sulfur, its unique nature, and its bio-generation [22]. Selenium is an essential micronutrient with a brain-specific physiology. While the brain is rather poor in selenium compared to other tissues, Kuhbacher et al. reported that selenium levels in the rat brain were the highest in hippocampus, cerebellum, brainstem and ventricles [23]. Biological functions of selenium manifest themselves via 25 selenoproteins that have selenocysteine at their active center, and the importance of selenium and selenoprotein for brain function, from antioxidant protection to neuronal signaling, is highlighted by Solovyev [24]. Selenium is later included in section 3.5 in the context of it being a 'metalloid'; strictly it is not a metal, but it shares certain properties with the metal elements.

Of most concern here are the late first row **transition metals:** iron, copper, zinc, and manganese, and while less abundant, chromium, cobalt, molybdenum, and nickel are also essential. With their rich chemistry, all of these were incorporated in living organisms quite early in evolution as essential for life. These elements are understood to be present in protein active sites as metabolic cofactors for structural and catalytic functions, but are increasingly also recognized for a second messenger role in cell signaling [4, 25]. As we will see later, there is a complex interplay between these metals in the life processes described by metallomics.

The essential metals must be obtained from the environment and appropriately bound or compartmentalized within the cell for use in biochemical pathways. They are then incorporated into proteins functioning in dioxygen transport, electron transfer, redox transformations, and regulatory control. They are essential for the growth and function of the brain, and become highly concentrated in grey matter with ageing [26], and play fundamental roles in white matter, for example in the myelination of axons. Their transport into the brain is strictly regulated by the brain barrier system, i.e., the blood-brain and blood-cerebrospinal fluid barriers [27]. The essential elements present a formidable challenge, in that their concentration range in any given compartment must be precisely regulated. Deficiency impedes biological processes, and excess can be toxic. Copper, for instance, is an essential metal that provides catalytic function to numerous enzymes and regulates neurotransmission and intracellular signaling. Conversely, a deficiency or excess of copper can cause chronic disease in humans [28]. Metallothioneins and related sulfur-rich chelators are understood to play important roles in metal ion homeostasis [29].

Once appropriated, metals must be directed to metalloenzymes or metal storage proteins within the cell. The precise regional, cellular and subcellular locations of these metals are increasingly objects of study. Transition metals can exist in many different forms within cells, including as free ions, coordinatively incorporated in biomolecules such as proteins, or in a labile association with low molecular weight species such as amino acids or glutathione, from which the metal ion could be released by changes in the cellular environment [30]. While metals show spatial time-averaged heterogeneity, there are also transient changes in concentration occurring as a result of exchange between metal-ion-binding species and labile metal ion pools within cells [4, 31]. Essential elements can undergo complex interactions with non-essential elements and other molecular components. In this context, it is no surprise that metal homeostasis is impacted in neurodegenerative disorders, but it is not yet fully determined in which diseases it is a causative factor as opposed to a consequence of other pathogenic processes.

There remain a large number of **non-essential elements** (metals and metalloids) in the periodic system of the elements that are not included in the periodic system of biology. Some of them are present at significantly higher overall concentration than the essential elements, while others became more abundant in life forms since the human influence in the Anthropocene [32]. While the bioactivity of some of these elements has positive effects on health, many non-essential elements

nevertheless are biologically reactive [33], in some cases both cumulative and detrimental to health. New applications and manufacturing processes expose animals and humans increasingly to a number of metals to which they have not been exposed to in the past, in particular those from the bottom part of the periodic system. Food chains and food webs amplify some exposures, which has largely unexplored effects for more recently employed metal ions [17]. The most hazardous of these build up in the biological food chain. Mercury, for instance, can thus affect the human nervous system and harm the brain. There are many issues of metal toxicity and environmental effects concerning toxic heavy metals (e.g. mercury, lead, cadmium) and other metals (e.g. aluminum, which in the so-called 'Aluminum Age', is now omnipresent in modern life). For instance, atmospheric deposition of mercury onto sea ice and circumpolar sea water provides mercury for microbial methylation, and contributes to the bioaccumulation of the potent neurotoxin methylmercury in the marine food web [34]. Different methylmercury species (compounds containing the CH_3Hg group) cross the blood-brain barrier and are highly neurotoxic. The element can thus affect the human nervous system and harm the brain. XRM of individuals poisoned with high levels of methylmercury species showed elevated cortical selenium with significant proportions of nanoparticulate mercuric selenide plus some inorganic mercury and methylmercury bound to organic sulfur. HgSe is a particularly stable and insoluble form of mercury with molar solubility product K_{sp} 10^{-59}. HgSe thus represents an inorganic, non-bioavailable, form effectively removing any mercury bound to selenide from involvement in biological processes [11].

Organisms must be able to sense systemic levels of metals in order to maintain homeostasis, to distinguish between essential and toxic metals, and must have mechanisms for minimizing the toxicity of both essential and toxic metals that are present in excess [3, 35]. Undoubtedly, since the Holocene/Anthropocene epoch, there must be many ways for non-essential elements to interfere, even cause havoc, in the delicate and complex chemical equilibrium reactions of biological processes as they evolved since the Great Oxygenation Event, ca 2.3 billion years ago. Most of these are unexplored at present. The scope and complexity of the potential interactions in-vivo are illustrated for the example of aluminum by Exley [36]:

"*Aluminum will also be bound by labile molecules in both intracellular and extracellular milieus and some of these interactions will involve its transportation as high- and low-molecular weight complexes throughout the body and, ultimately, the excretion of aluminum from the body. The potential for aluminum to interact with and to influence so many biochemical pathways means that the symptoms of its toxicity could be deficiency or sufficiency, agonistic or protagonistic, and any combination of these and other physiology-based events".*

Many metal ions (essential or non-essential) are understood to play critical roles in disorders of the central nervous system including AD, Parkinson's disease (PD), amyotrophic lateral sclerosis (ALS), Multiple System Atrophy (MSA), prion diseases, and others [15, 37-40]. For example there is evidence of brain copper dysregulation in AD [38]: changes in the distribution of copper has been linked with various aspects of the disease process; protein aggregation, defective protein degradation, oxidative stress, inflammation and mitochondrial dysfunction. Although AD is a multifactorial disease that is likely caused by a breakdown in multiple cellular pathways, copper and other essential metal ions such as iron and zinc play a central role in many of these cellular processes [28]. The role in neurodegenerative disorders of these essential metals, and of those acquired through environmental exposure, requires better understanding [36, 41].

Understanding the complexity of metallochemistry in the living brain is critical to designing appropriate therapeutic interventions. For example, combinations of iron, zinc, copper and aluminum have been shown in-vitro to influence the formation of amyloid fibrils found in a

pathological hallmark of Alzheimer's disease (AD) in a manner which may have consequences for metal chelation therapy [42], and the potential to use iron chelators as therapy to delay PD and related disorders is being explored in clinical trials [43].

Metal-containing drugs are used for the treatment of diseases, such as cytostatic platinum derivatives against tumors, lithium as mood stabilizer, gold complexes against rheumatoid arthritis. A series of lanthanide metals, such as gadolinium complexes, are used as contrast agents in medical imaging techniques. More recently iron oxide nanoparticles that have superparamagnetic properties (SPIONs) have been exploited as contrast agents in magnetic resonance imaging (MRI), where the local magnetic field of the nanoparticles has a significant effect on the magnetic relaxation properties of the surrounding tissue. Approaches include the direct injection of coated SPIONs to demarcate for example into brain tumor tissue for pre- and post-operative identification, and the introduction into the brain of SPION-laden neural cells to enable tracking of tissue regeneration [44].

3. Chemical imaging and imaging analysis

In order to fully appreciate the potential of X-ray chemical imaging methodologies for chemical imaging of biological materials we need to compare their characteristics with those of the "ideal microscope" [45]. In an ideal world, data from one single microscope would be able to yield sufficient information to build a complete picture of a cell in its native (living) state. In reality this is an impossible dream [46]. Different microscopic techniques have particular unique imaging characteristics. Based on particular methodologies, we may discern infrared, visible, UV or Raman microscopy, XRM, electron microscopy, particle induced X-ray emission, mass spectrometry imaging, fluorescent labelling methods, proximal probe microscopies that are capable of generating data within a well-defined window of spatial resolution and information content. The combination of several modes of observation in a single instrument is advantageous. In recent years, correlative microscopy, combining the power and advantages of different imaging systems, incorporating light, electrons, X-ray, nuclear magnetic resonance (NMR) and so forth, has become important, especially for the study of biological materials [47]. Among all the possible combinations of techniques, light and electron microscopy are historically prominent. This review will highlight, amongst others, the possibilities of X-ray imaging techniques in combination with light and electron microscopy and mass spectrometry imaging for more comprehensive analysis of the material complexities of the brain.

3.1. The ideal chemical microscope for biological materials

Techniques for *in situ* metal imaging analysis depend on three key properties: spatial resolution, sensitivity, and selectivity. Spatial resolution and sensitivity are negatively correlated, they are connected since the absolute detection limits are defined by the amount of analyte being sampled in a given two-dimensional (2D) pixel or a three-dimensional (3D) voxel. Selectivity concerns the ability to determine the metal's chemical form, oxidation state, coordination environment or association with specific proteins or other molecular structures [16, 48].

The most important characteristics of the ideal microscope are summarized in **Figure 1**. The "**spatial resolution**" at the left in the figure determines the 2D or 3D spatial discrimination level of the measurements. Recent evolution of synchrotron X-ray imaging methods has achieved in routine microscale chemical imaging and a spatial resolution of 10 nm or better, close to the supramolecular interaction level of molecular assemblies in cells. By contrast, laboratory scale instruments combining absorption computed tomography CT and XRF-CT have been developed with spatial resolution reaching 20 μm [49].

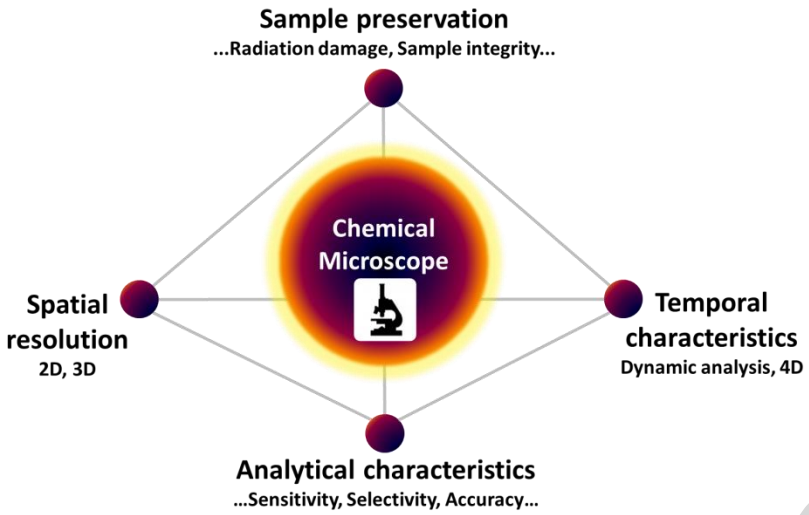

Figure 1: The different characteristics that determine imaging analysis, adapted from Scherf and Huisken [45].

The term "**analytical characteristics**" determines the analytical information that is derived from the measurements. Just like other methods in analytical chemistry, chemical imaging analysis is characterized by a number of quality criteria such as sensitivity, specificity, and accuracy (exactness). Most analytical imaging techniques allow for qualitative information; quantitative imaging is often difficult, mainly as a result of matrix effects [50]. Accuracy and consequently quantitative imaging analysis with X-ray imaging tools depend on issues such as linearity of response, the dynamic range of the response curve and the extent of matrix interferences and other measurement artefacts; they will be covered further in this review. We should also distinguish analytical coverage (elemental, molecular, structural and so forth) and the data-generating ability (multi-spectral, hyperspectral, and so forth). The detection limit is determined by the signal-to-noise ratio of the spectral measurements. A higher spatial resolution yields a reduced sample size and hence, a reduced signal. With SR-XRF, the absolute detection limit is as low as 10^{-18} g for transition elements such as of Fe, that can be detected within a cellular structure that has a diameter of 90 nm [13]. Finally, the selectivity determines the potential of a method for discrimination between molecular form, oxidation state, and coordination environment (speciation). There are a number of other characteristics that need to be considered, such as speed of the analysis, degree of automation, the cost of the infrastructure or accessibility of the instrumentation and so forth. As discussed in section 6, the facility time available for XRM at synchrotron sources exceeds demand.

"**Sample preservation**" (sample integrity, sample health), a particularly important factor for biomaterials, is connected with the way the sample is able to tolerate the measurement process without deterioration. It is affected by factors including the vacuum conditions, hydration state of the sample, temperature, and dose received from the X-ray beam.

Minimizing the radiation dose for a given image resolution and contrast is a primary challenge for XRM. Radiation damage is dose-dependent and alters and subsequently destroys the sample and drastically limits the applicability of any imaging method. SR beamlines enable high-resolution applications but radiation damage becomes more pronounced as the spatial resolution is pushed to smaller values. For delicate biological samples, minimizing the applied dose for a given image resolution is a primary challenge, and biological samples are heterogeneous from the perspective of radiation damage. Resilience is heavily dependent on the properties of the material under investigation and the sample environment. X-rays are less damaging than most other projectiles used

in analytical beam techniques. With hard X-rays of 13.8 keV, 3D tomographic reconstructions with a total dose of 1.6 x 10^5 Gray (J/kg) were documented [51]. Such doses allow multimodal hard-X-ray imaging of a chromosome with nanoscale spatial resolution without detectable radiation damage between two successive scanned images [52]. For analysis of metal ions in brain tissue, it is critical to understand the chemical (and in some cases mineral) modifications to metal elements as a result of the received dose [53].

Sample history prior to measurement is as important as the analytical environment; some XRM methods may be used to image live cellular material, but the majority of studies utilize archived brain tissue or cells that have been chemically fixed, frozen, and/or dehydrated prior to measurement. The effect of sample processing on tissue integrity and retention of trace metals in mammalian cells and tissues is an important area of study [54, 55].

At room temperature, wet specimens are damaged by impinging radiation due to primary bond breaking as well as hydrolysis of water, so that they suffer from shrinkage as well as material diffusion. Dehydration conveys increased robustness against radiation damage but a significant breakthrough towards accurate imaging of subcellular structures and elemental distributions was achieved by rapidly cooling the fully hydrated sample to a vitrified state and imaging the samples under frozen-hydrated conditions [56]. Such biological samples have better preserved local structure and elemental composition than dehydrated ones [9].

"**Temporal characteristics**" are important in two respects. First, scanning for the purpose of 2D and 3D imaging analysis is an inherently slow process. It comprises economic factors such as speed and cost. Apart from this economic factor, the total measurement time to generate an image also dictates the scope for dynamic measurements of time-dependent processes. Sensitive approaches are required to follow fluctuations in normal metal homeostasis that accompany processes of development, differentiation, senescence, stress response and so forth, or to acquire knowledge about the redistribution of metals and trace elements accompanying the development of different diseases [57]. Ahmed Zewail, Nobel laureate for chemistry in 1999, summarises how space-time applications, particularly 4D electron microscopy but also other imaging methods can be exploited for such work [58]. 4D electron microscopy is used for studying picosecond dynamics, but even at orders-of-magnitude longer time scales the study of time-dependent processes by XRM has potential to provide important insights. That metal ions can be mobilized via labile pools in cells, which are tightly regulated by complex systems, indicates that in addition to spatial heterogeneity, there is an important temporal component that is influenced by specific cellular events. Exploring the metal content with high spatial and temporal resolution requires advanced analytical tools and techniques [30]. There have been advances in imaging metal ions in living cells with high spatial and temporal resolution using optical fluorescence microscopy, and spectroscopic methods (including Fourier transform infra-red and small angle X-ray scattering) to study processes such as conformational changes to proteins when they undergo metal binding, are discussed elsewhere [15]; dynamic 4D XRF imaging methods are not presently established.

3.2. Methods for imaging analysis of biological samples

Over the past years, there has been rapid improvement in sensitivity and spatial resolution for multi-element (panoramic) bio-imaging of metals, with different methods now providing micron to sub-micron spatial resolution, and with detection limits from 0.1 to 100 $\mu g.g^{-1}$. The existing bio-Imaging methods that are used at present are based on: (1) mass spectrometry; (2) "beam" methods employing (laser) light, electrons, X-rays or energetic particles to measure characteristic radiation; or

(3) methods employing metal-selective probes [30]. Each method has its own advantages and limitations, such as the ability to deliver reliable quantitative analytical results, and the overall cost of the use and accessibility of the instrumentation.

Of the methodologies that are based on excitation of the lower electronic shells, the most powerful is achieved by the combination of high spatial resolution with high sensitivity XRM. This requires instrumentation that is not readily accessible. Electron excitation in electron microscopy techniques (primarily scanning electron microscopy, electron probe microanalysis, and transmission electron microscopy) is orders-of-magnitude less sensitive for elemental analysis [48]. Proton or other heavy ion beam techniques approach the sensitivity and spatial discrimination levels of XRM, but rely also on complex and not easily accessible instrumentation [59]. Mass spectrometry Imaging (MSI) techniques have the unique advantage of being able to measure isotope ratios. For elemental analysis, dynamic secondary ion mass spectrometry (D-SIMS) combines spatial resolution down to 35 nm with attogram (or less) detection limits but is limited to the simultaneous measurement of only 5-7 isotopes in the major instrument used for bio-analysis, the Cameca NanoSIMS [60]. Laser ablation inductively coupled plasma mass spectrometry (LA-ICP-MS) has detection limits for most elements approaching ppb levels, but is limited to a spatial resolution of the order of the µm. This is within the realms of sub-cellular neuronal imaging [61, 62]. The sensitivity of LA-ICP-MS can be an order-of-magnitude superior to that of many SR XRM techniques [40], but this is being challenged by advances in XRM beamline development. Compared with LA-ICP-MS, µ-XRF can offer higher resolution (tens of nanometers), although the respective merits of the two techniques depends on the elements being studied, the science question being addressed, and sample handling constraints [63].

3.3 Imaging analysis in biology and medicine

Metals are heterogeneously distributed within biological materials. Understanding the functioning of normal and pathophysiological processes requires imaging techniques at different scales of spatial discrimination. As illustrated schematically for the brain in **Figure 2**, the constituent material can be considered at three levels of spatial resolution: that of the organ, the tissue architecture composed of individual cells, and the cell and its intercellular structures (organelles). Tissues are complicated assemblies of multiple interacting cell types that communicate with each other to achieve physiological states. At the highest level, imaging of metal species and compounds in biological materials requires nanometer spatial resolution to match the intracellular complexity and to visualize interactions at the molecular and supramolecular level. Metals are found in high concentrations within structures where they react, particularly in organs with high metabolic activity such as the brain. Within cells, metals are localized according to need. For example: mitochondria contain high levels of iron in Fe-S clusters and products of haem synthesis; the nucleus is rich in zinc finger proteins essential for gene transcription; and the Golgi complex is a major regulator of cellular copper levels [48, 64].

For metal imaging, sub-ppm (i.e. attogram or lower) detection limits for a wide range of elements are required. To obtain a deeper understanding of complex biological processes at tissue or even cellular level, analytical techniques with spatial resolution on the nanometer scale are needed. This problem is tackled by the application of confocal and super-resolution imaging tools. Another problem is that biological soft tissue is almost transparent and weakly scatters X-rays, which hampers the observation of tissue structure and composition. Biological problems cannot normally be addressed on the basis of the distribution of metals or metal species in the specimen alone. Additional and complementary contrast mechanisms are needed. In the past, such contrast enhancement was commonly achieved using heavy elements as a contrast medium. However, with XRM, the distribution of density contrast in the sample can be obtained from quantitative phase

reconstruction schemes along with the reconstructed volumes, shapes and topologies [51, 65, 66]; In this way the need for sectioning and staining of the specimen can be avoided.

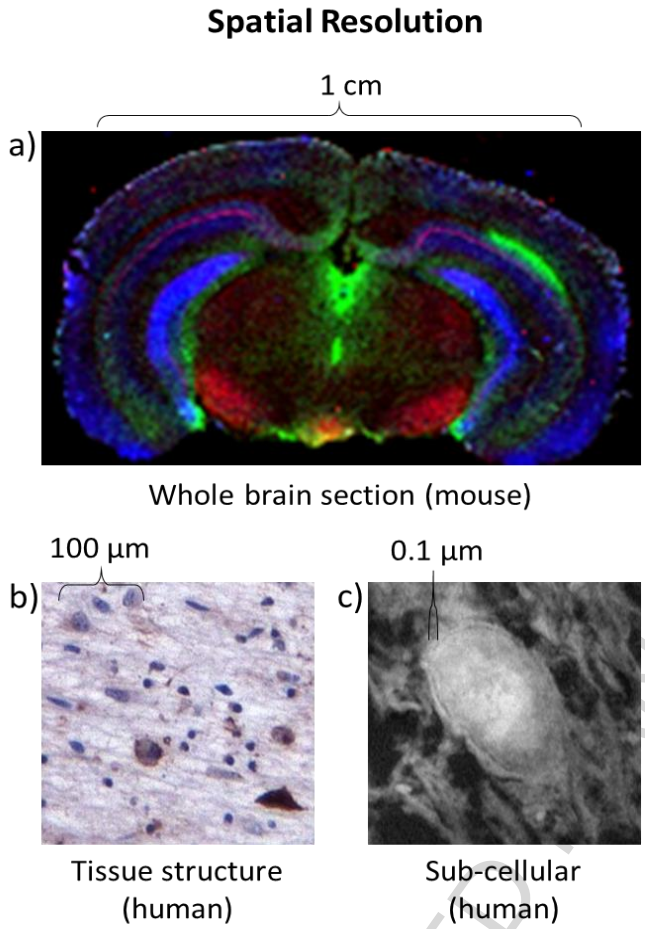

Figure 2: Spatial resolution in chemical imaging of the brain, inspired by Hare et al [48]: a) X-ray fluorescence imaging of transition metals in a coronal mouse brain section (mapped at the I18 beamline, Diamond Light Source, tissue courtesy of J.R. Connor and A.M. Snyder, Penn State), b) ferritin-stained tissue from the human basis pontis (adapted from Visanji et al [67]), c) STXM oxygen K-edge speciation map of resin-embedded human putamen, courtesy of J. Everett, V. Tjendana-Tjhin, J.F. Collingwood, and N.D. Telling, using data obtained at the ALS beamline 11.0.2, tissue provided by L.N. Hazrati on behalf of the Canadian Brain Tissue Bank under UK ethical approval 07-MRE08-12.

3.4 Metals in biology

Metals are present in cells and organisms as free ions, or bound to various molecular entities. Around one third of all structurally characterized proteins are metalloproteins. Bound metal ions, or co-factors, play an essential role in the structure–function relationship of proteins and other bio-molecules. Biologically essential metals, as well as those without known biological use or which are known toxins, may be harmful if incorrectly metabolized. Thus, sophisticated interdependent systems are in place throughout the body and the compartments of the brain to regulate metal ion metabolism, to ensure the essential metals are available as required, and to prevent or mediate toxicity arising from loss of homeostasis [68].

Measuring and mapping transition metal elements such as iron, zinc, copper and manganese by simultaneous acquisition is a critical step toward learning how they are utilized for biological

processes, some of which are unique to the brain. It is also critical to understanding the damage metal species can cause under certain circumstances where metabolism is altered and homeostasis disrupted. Exploring the contribution of disrupted metal ion metabolism in diseases affecting the brain, and designing interventions to limit or prevent metal-ion-mediated damage, requires careful analytical study supported by robust models of disease. Certain diseases are demonstrably caused by exposure to a particular metal. For example, exposure to manganese causes manganism, a syndrome similar to parkinsonism [41, 69]. In some diseases faulty metal metabolism is a primary factor, such as in neuroferritinopathy or aceruloplasminaemia [14, 35]; in other neurodegenerative disorders such as AD, PD, and MSA to name but a few, there is evidence for altered metabolism of metal ions contributing to the disease process but there is much still to understand [35, 64, 67, 70, 71]. For example, within the brain in MSA there is evidence of excess intracellular iron storage accompanied by a deficiency in the cellular export protein ferroportin [67]. Such scenarios may results in an effective deficiency of the element in a given cellular compartment, even though bulk analysis of a tissue sample from the affected region will indicate the element is present in excess. Other non-essential elements such as lead or mercury are recognised neurotoxins and can cause serious brain damage where there is a route for the toxic element into the central nervous system.

3.5 Metals in the brain

The brain has a unique chemical composition and reactivity at the molecular level. The requirements arising from cognitive and motor functions result in its having the highest concentration of metal ions in the body and the highest per weight consumption of body oxygen [1], a side-effect of which is its heightened vulnerability to oxidative stress damage. Transition metals such as copper, zinc, iron, manganese, and cobalt are key cofactors in a wide range of brain cell functions, including cellular respiration, antioxidant removal of toxic free radicals, and oxygen delivery to brain cells. They are also cofactors for cell signaling at synapses. Even minor disruption to, or errors in, the regulation of biometals can impact cell function and, ultimately, neuronal survival [72]. As opposed to most other trace elements, which are coordinated to protein ligands, selenium is covalently bound. As a component of the amino acid selenocysteine, it is incorporated in several selenoproteins which play important roles in brain development and metabolism [23, 24].

Multiple abnormalities occur in the homeostasis of essential endogenous brain biometals in a wide variety of disorders, including epilepsy and neurodegenerative disorders such as AD, PD, ALS, MSA and Huntington's disease. This includes abundant elements such as calcium, the transition metals, and trace elements such as the metalloid selenium. Metal accumulation is frequently associated with microscopic insoluble protein deposits in the proteinopathies, and can be deficient in cells and within cellular compartments. Therefore, it is essential to study them on the microscopic level [25, 50].

Mineralization of certain metals, including iron and calcium, is inherent to physiological and certain pathophysiological processes (e.g. the formation of ferrihydrite cores in the iron storage protein ferritin, and the deposition of calcium in brain tissue in the rare disorder Fahr's disease, respectively). In recent work from Maher and colleagues [73], it is suggested that magnetite nanoparticles observed in post-mortem human brain samples originate from air pollution, and it is noted that similar nanoparticles have been associated with AD pathology [74]. Indeed, evidence for magnetite deposits associated with amyloid pathology has previously been demonstrated by a range of analytical techniques including μ-XAS in tissues surveyed by μ-XRF [75, 76]. However, it was assumed that the magnetite formation was endogenous; potentially a consequence of an interaction between iron stores and aggregating amyloid [77]. The scope for nanoparticulate iron oxide to stimulate excess free radical production is documented elsewhere [78], and although mishandled iron in the

brain may contribute to the toxicity of the hallmark amyloid plaques in AD, there is not yet enough known to establish whether an external source of magnetite from air pollution may be a factor in the disease.

The interplay and complexity of metal ion metabolism is routinely underestimated, with analytical and conceptual constraints leading to many studies where a metal element is studied in isolation. There are the elements known to be essential to normal brain function, such as calcium, copper, zinc, or iron, where aspects of their metabolism are interdependent, and in addition there are elements such as aluminum which are understood to be non-essential but which can amplify catalytic pro-oxidant reactions involving essential metals [79]. This interdependency is critical in conditions of both deficiency and excess. For example, the loss of the main copper transport protein, ceruloplasmin, appears to be responsible for derailing iron homeostasis in aceruloplasminaemia [35], and there is evidence for localized brain iron accumulation in Wilson's disease, which is primarily a disorder of copper accumulation (including in the central nervous system) [80]. This presents a significant analytical and computational challenge. Despite advances in the development of models of brain metabolism, there is an inevitable dependency on empirical data to determine the impact of interventions such as chelation treatments. Chang recently created an analogy for metallomics in which the essential metal elements are compared with the different instrumental parts in a symphonic work. Describing or modifying the harmony of the orchestration cannot be achieved by following a single instrument (one element); it instead invites comprehension of the contributions from the full orchestra (i.e. the interplay of all contributing elements, essential or otherwise) [4]. Overall, the power of X-ray microscopy techniques is that they offer an unparalleled combination of sensitivity, specificity and spatial resolution to access simultaneously this broad spectrum of metal elements.

4. X-ray microscopy imaging

X-ray imaging provides a set of unique tools for studying metal distribution in situ in biological materials. Quantitative single cell and subcellular measurements of metals inform us about both the spatial distribution and cellular mechanisms of metals within the cellular microenvironment of many different tissues and cell types including the brain and spinal cord of the central nervous system. For proper evaluation, 2D and 3D metal concentration distributions need to be correlated with the sub-cellular morphological and functional components. A major factor in the development of synchrotron–based X–ray imaging is the coherence of the synchrotron beams, which enables higher sensitivity and a spatial resolution no longer affected by optical artefacts due to lens systems when exploited as a full-field microscopy technique.

The potential of X–ray imaging that resulted from its penetrative character was obvious since its inception. Almost immediately after the discovery of X-rays by Wilhelm Conrad Röntgen, they were used for macroscopic imaging of the human body giving absorption imaging contrast according to the density distribution discriminating between soft tissue and bone structure. Their development into a practical analytical technique for elemental analysis, however, has been slow due to the lack of sufficiently intense X-ray sources. It was the development of synchrotron radiation (SR) from electron storage rings in the last quarter of the twentieth century that provided the necessary flux and brightness for microscopic and sub-microscopic applications. While X-rays produced in X-ray tubes spread out almost isotropically as they travel away from the source, SR is emitted with high directionality. The major goal of X-ray optics is to concentrate X-ray photons into a small area and

thus gain in flux compared to methods relying on geometrical confinement with pinholes or slits. Their very low emittance combined with high brilliance allowed the development of efficient focussing devices used in XRM and led to a dramatic increase of the use of SR–based X–ray imaging for obtaining information on density, chemical composition, chemical states, structure, and crystallographic perfection.

The SR spectrum that is generated in synchrotron radiation sources ranges from the IR to several tens of a keV. Several types of monochromators can be used to select particular X-ray energies for imaging experiments. The minimum time resolution achievable using X-rays from storage rings is limited by the X-ray pulse width to ~100 ps.

There is a variety of X-ray analytical techniques that can be used as contrast in X-ray microscopy. Through their ability to scatter and refract, X-rays provide sensitive ways to visualise structural and compositional changes. First, there is absorption as a result of photoionization in the lower electron shells. Absorption imaging contrast varies with Z^4 and, as such, provides a crude composition-dependent imaging tool. The distribution of elemental constituents can be analysed inside a sample by measuring X-ray fluorescence radiation, while X-ray absorption measurements around an electron binding energy edge can provide the chemical state and the local chemical environment of given atomic species. X-ray diffraction can be used to obtain information about the local nanostructure. As opposed to conventional absorption imaging, which reflects the local amount of energy deposited in the sample, phase contrast mode techniques are sensitive to the variation of the refractive index in the sample similar to the phase contrast mode of a light microscope. Refractive index variations lead to the bending and scattering of the X-ray wavefront which can be detected without depositing substantial energy in the sample [81]. Phase contrast projection tomography substantially improves soft-tissue contrast as we will discuss further in section 4.5. Application of such methods allows a large field of view in all spatial dimensions at sub-cellular resolution without the need for sectioning or staining [51]. Imaging of absorption, fluorescence radiation and phase contrast each give additional information about the sample. In this way, in addition to determining chemical composition, X-ray imaging provides valuable complementary information about the nature of the sample such as density and structure.

The large penetration depth of X-rays (ranging from a few microns to a few mm for a biological matrix, depending on the excitation energy) offers possibilities for simple preparation procedures and more versatile *in situ* observations in controlled environments. X-ray imaging is suitable for the micro-analysis of delicate biological samples close to their natural wet state, as imaging does not necessarily have to be performed in a vacuum under cryogenic conditions (see section 6). Under certain conditions, where radiation damage can be appropriately controlled, it is therefore possible to undertake live cell imaging with certain methods.

Due to the microscopic size of the primary X-ray beam and its high flux (perhaps 10^{10} - 10^{11} photons/s), radiation damage may be caused by absorbed X- ray photons depositing energy directly within the sample, mainly causing inner orbital electrons to be ejected due to the photoelectric effect [82]. Radiation damage from both hard and soft X-ray beams must be taken into account in any experiment, although as a rule of thumb it will be less significant than from electron beam exposure. Damage to the organic material, which can result in mass loss where the beam has interacted locally with the tissue, might be observed. Determining the dose received by the sample is also important to determine if the metal ions within the tissue may be photo-reduced [53]. If beam-induced changes to the metal ion chemistry are potentially so rapid that they cannot practically be observed, then the priority is to ensure an identical protocol is followed for all sample groups such that like can be compared with like.

For more detailed information on the physics of X–rays and on their interactions with matter, we refer to the handbook of Als–Nielsen and McMorrow [83]. Bilderback et al. give an excellent review of how third-generation synchrotron light sources have made their mark on twentieth century science and pave the way to continuing accelerator developments into the twenty-first century [84]. A general overview in which X-ray imaging methods are compared with other chemical imaging analysis methods is given by Adams and Barbante [85], and there are various reviews considering aspects of X-ray imaging in biology and medicine, with some examples provided here [15, 48, 57, 68, 86].

Optimum conditions of spatial resolution and sensitivity can only be realized with X-ray sources from third generation storage rings. A significant feature of so-called third-generation storage rings is that they are specifically designed to obtain unprecedented intensity and brilliance. Third-generation sources become operative in the early 1990s and were designed on the basis of experience gained during the construction of earlier particle accelerators. Most of these large-scale facilities are operated as open-access laboratories for external users. Long-established large synchrotron facilities include the ESRF (Grenoble, France), the Advanced Photon Source (APS) at the Argonne National Laboratory (USA), and SPring-8 in Harima (Japan). More recent examples include the Diamond Light Source (UK), Soleil (Paris, France), and DESY, PETRA III (Germany) and the Australian Synchrotron; in spring 2016, 47 synchrotrons were available internationally as documented at the user resource www.lightsources.org and more are under construction. At some SR facilities, beamlines devoted to biological research have been constructed. Among them is the Bionanoprobe, a hard XRF nanoprobe with cryogenic capabilities at the APS. The Bionanoprobe beamline provides a spatial resolution of 30 nm for 2D XRF imaging with cryogenic sample environment and cryo-transfer capabilities, dedicated to studying trace elements in frozen hydrated biological systems close to the “natural state” [56]. Many third-generation synchrotrons deliver output from the ring of 2–3 GeV, with the most powerful operating at 6–8 GeV. Access to such facilities is on the basis of research proposals and is very competitive. We comment further on access conditions in section 6.

The continuous gain in brilliance of SR sources over the past three decades and the resulting advances in focussing optics currently provide a lateral resolution well below the sub–micrometer range while maintaining high detection sensitivity. Spatial resolving power of 10 nm has been demonstrated with soft X-rays [87], and is expected to become more routinely available in the near future. In practice the highest achieved resolutions are presently in the 20 – 30 nm range. Scanning X–ray Fluorescence (XRF) and X–ray Diffraction (XRD) based on third–generation SR sources are now routinely performed at well below the 1 µm scale and there is a growing interest in sub–µm photon beam sizes to investigate the nanoscale compositional and structural organisation of material.

Recent developments in laboratory X-ray microscopy systems, both commercial and in-house, can provide similar analytical information. For example, a custom-built instrument offers a laboratory-based method for XRF mapping of iron and other elements in human brain tissue [39]. While some commercial XRF imaging systems now provide spatial resolution and sensitivity sufficient to image some of the most abundant elements in biological systems, the limited spatial resolution, sensitivity, and versatility compared with synchrotron X-ray instruments limits the stand-alone systems for most bio-imaging applications even at the highest magnification level.

4.1. Methods for X-ray Microscopy

The X-ray imaging methods can generally be subdivided into two modalities: techniques which focus on the chemical composition (e.g. X-ray fluorescence for elemental analysis and absorption spectroscopy for chemical state “speciation” analysis) and techniques which are designed to obtain

structural or morphological information (e.g. absorption or phase contrast tomography) on a sample. For the purpose of imaging metal species and compounds in tissue, XRF and X-ray absorption spectroscopic (XAS) methods based on the use of tuneable energy X-ray beams of (sub)micron dimensions represent very powerful analytical techniques for non-destructive elemental/chemical-state analysis with the possibility to perform spatially-resolved measurements down to trace (ppb) concentrations.

We need also to distinguish two working principles of X–ray microscopes: full–field microscopes, and scanning microscopes. In full–field microscopes the whole field of view is simultaneously imaged onto a detector plane, while in scanning microscopes a focussed beam is raster-scanned over the sample, collecting each data point separately. In the latter type of microscope an integrating X–ray spectral detector can be used. Full–field, non-scanning X-ray imaging techniques can shorten the imaging time drastically, but a spatially integrating X–ray detector can be used. In full–field microscopes a more costly spatially-resolving imaging detector is required such as a CCD or pixel-array (colour) detector. Scanning systems require sophisticated, nanofabricated X-ray optics as lenses. Scanning, full-field and lens-less X-ray microscopy techniques have been developed, with a spatial resolution ranging from around 25 nm to 100 nm. A distinction must be made between high energy (hard) and low energy (soft, sub-keV and above) X-rays but the difference between these two operational regimes is not well defined. Typically, it is considered that hard X-rays are those with energies greater than around 10 keV. They are the excitation mode for most multi-elemental metal imaging as they give rise to photo-ionization in the K- and L-electron shells of the majority of biometals.

4.2 X-ray fluorescence imaging

Microfocus X-ray fluorescence (μ-XRF) imaging provides a unique tool for studying the distribution of multiple metal species in biological samples through simultaneous acquisition of the signal from all the detectable elements in a single measurement. It is performed at spatial resolutions ranging from microns to tens of nanometer resolution at specialized “microfocus” and “nanofocus” beamlines at state-of-the-art synchrotron facilities.

Micro-XRF is a sensitive elemental analytical technique; it almost matches the sensitivity of laser ablation inductively coupled mass spectrometry (LA-ICP-MS) [63]. As soon as an atom becomes ionized by an electron, an X-ray photon or a high energy particle interaction, it gives rise to a quick reorganization process in which X-rays are emitted. This core shell ionization underlies XRF mapping and other spectroscopic methods such as particle-induced X-ray emission (PIXE) and scanning electron microscopy/energy-dispersive X-ray analysis (SEM-EDX). Electron excitation does not offer the required sensitivity for the mapping of metals in biological samples as the result of intense Bremsstrahlung background [48]. Micro-PIXE is a valuable ion microprobe technique that has often been successfully used for 2D elemental mapping and quantitative trace element analysis of biological and environmental samples [88].

An attractive feature of XRF is its conceptual design simplicity (see **Figure 3**). It consists of a mechanical sample stage with computer-controlled high precision micro stepping motors for x, y and (optionally) rotational movement of the sample, one or more detectors for the measurement of the fluorescent radiation, different visualization tools for observing the sample and, finally, a range of diagnostic and control tools. Most applications are in a scanning mode based on imaging lenses that focus the exciting radiation (the incoming primary beam) on a particular location of the object of analysis. Various methods are used to micro- or nano-focus the X-ray beam, including the Kirkpatrick-Baez geometry which utilizes two glancing-angle concave mirrors, the curvature of each being

adjusted to define the beam profile at the focal point [89]. The focused X-ray beam impinges on the sample and X-ray spectra are retrieved as the sample is step- or raster-scanned, typically in a plane at 45° to the beam path, so as to allow systematic measurements over a given area. The fluorescence radiation spectrum is then measured with a suitable energy-discriminating detector. The exciting radiation is either polychromatic (white), or monochromatic at $\Delta E/E = 10^{-2}$ for normal fluorescence applications at reduced flux but increased signal-to-background and better detection limits. High resolution scanning at $\Delta E/E = 10^{-4}$ is used for scanning around the absorption edges of selected elements. Normally the X-ray beam energy can be selected over a given energy range.

The sample on its stage mount is typically rastered in the x, y plane (the schematic above is viewed along the y-axis), and adjustment along the axis of the beam is performed to bring the sample to the focal point. The polarization of the incident radiation can be used to reduce the relative contribution of scattered radiation reaching the detector as scattering cross sections are dependent on the polarization, while fluorescence radiation is not. Performing measurements in the plane of the SR source increases the signal-to-background ratios by up to two orders of magnitude.

One or more detectors capture fluorescence spectra over a solid angle from the sample and output these to files with the accompanying x, y coordinates for each point or 'pixel' where the X-ray beam is incident. Plotting the fluorescence intensity for one or more elements allows construction of an image of metal distribution; the field of view is determined by the chosen number of steps in x and y. For the measurement of elemental distribution maps, μ-XRF typically depends on one or more of the following semiconductor detectors for measurement: conventional Si(Li) detectors, intrinsic Ge detectors, or a Silicon Drift Detector (SDD). The limited energy resolution of the energy-dispersive detection yields complicated spectra with multiple spectral interferences. Spectral deconvolution methods are used to obtain net X-ray intensities of the elemental components. Also, high count rates must be adequately taken into account, e.g. by using digital pulse processing.

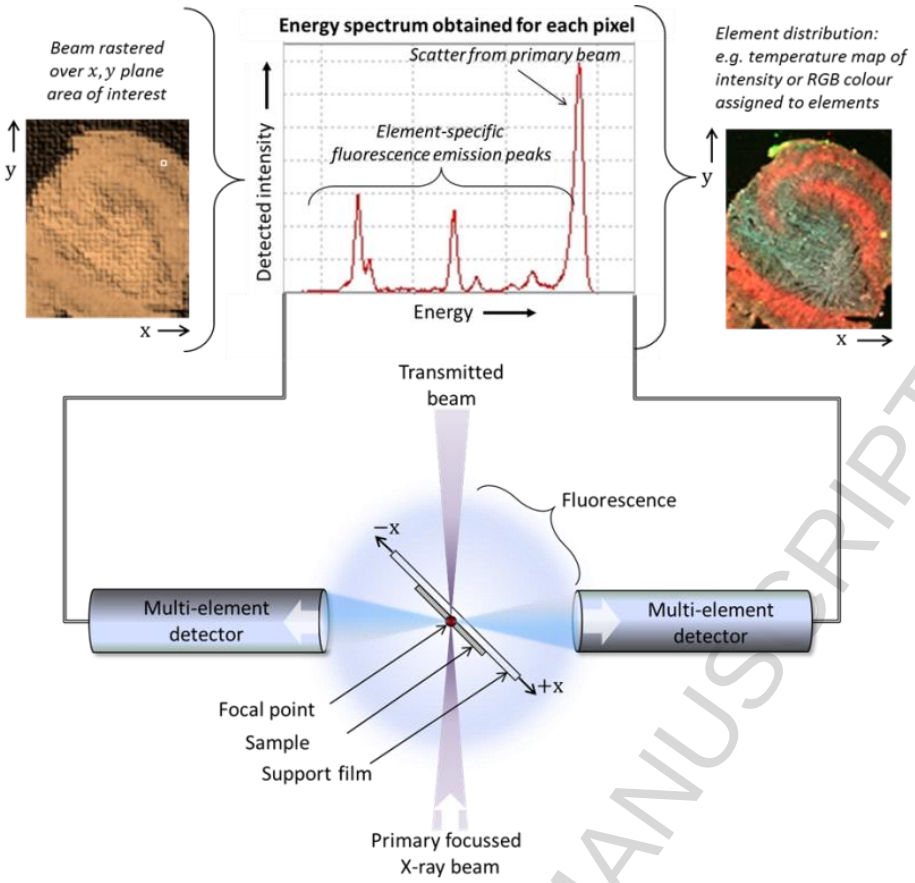

Figure 3: μ-XRF analysis using a focussed beam (the primary beam) of X-rays at an energy selected to stimulate fluorescence emission from the elements of interest.

A drawback is that such a microprobe is limited to collecting only one pixel at a time (step-scanning) or via continuous movement of the stage (raster-scanning), making applications in imaging a time-consuming process. While continuing improvements in software and hardware have significantly improved the efficiency of XRF imaging experiments over the past decade, there are promising developments with true imaging microscopes that collect all the pixels simultaneously with spectrally integrating CCD cameras. These have scope to be much faster for imaging at micron-scale resolution, and while the need to incorporate reflective optics places constraints on the field of view, they provide a rapid method to identify regions of interest (ROI) in a sample prior to detailed analysis [90]; these colour X-ray cameras are increasingly being used.

4.3 XRF calibration, quantitative analysis

Imaging analysis is normally achieved by relating the intensity of a particular spectral feature to the concentration of one or more analytes in the sample. Most chemical imaging methods provide for qualitative information; quantification is difficult and only available for a few methods. Many applications rely on reliable identification of metals and identification of concentration changes with localization.

Extracting quantitative information is rendered difficult due to matrix effects and other instrumental factors affecting the measurements; these are particularly important for samples with a high degree of complexity and heterogeneity, such as biological materials. Ignoring self-absorption in the sample, which is normally appropriate for thin biological samples, the characteristic fluorescence signal is

linearly proportional to the concentration of the corresponding element. Because the organic material is transparent to hard X-rays, the observed absorption can be assumed to be due solely to the metals. XRF (or emission) forms the basis of the most accurate chemical imaging tools [91]. Several beamlines devoted to metrology at synchrotron radiation facilities enable performance studies with these powerful sources, and aim at improving the accuracy of the analysis. While the reliability of the quantitation depends on the relative uncertainty of the atomic fundamental parameters and on well characterized X-ray sources and detectors, metrology-conform reference-free X-ray spectrometry is possible using synchrotron radiation [66, 92].

Quantitative assessment of the spatial distribution of metals in brain tissue is of significant interest to neuroscientists, given the current interest in modification of brain metals by chelation as novel treatment strategies for common neurodegenerative disorders, such as PD and AD [25, 93], as well as understanding the role of specific metals in pathogenesis and the scope for utilizing changing patterns of metal ion distribution in early diagnosis [35, 94].

Synchrotron radiation μ-XRF is considered the most reliable method for non-destructive quantitative trace element imaging of biological systems at sub-μm spatial resolution. Potentially, it is a reference–free imaging method and, as such, a tool for validating other elemental imaging methods and for the calibration of standard reference materials. In practice, many facilities are able to quantify the distribution of elements throughout a sample, but not all of them are optimized to determine the absolute concentration of the elements in a heterogeneous biological material with varying thickness and density. The main drawback of the technique resides with the difficulties of access to the instrumentation, highlighting the need for continued long-term investment in, and maintenance of, world-class synchrotron facilities. The other prominent method for quantitative trace elemental imaging analysis is LA-ICP-MS; this method is necessarily destructive of the sample material being analysed.

For a fully theoretical conversion of the intensities of the characteristic lines of the elemental constituents into their mass fractions, the fundamental parameters approach first developed by Shermann in 1955 is now commonly followed [95]. However, due to the relatively large number of parameters to be known, a rigorous theoretical approach is fairly difficult and various simplifications have been proposed. Surowka et. al. describe the use of several semi and fully-quantitative methods to correct for the absorption effects for dried substantia nigra tissue specimens on thin Si_3N_4 substrates (see section 6) using either the membrane Si transmission signal or the intensity of incoherently scattered primary X-ray radiation [96].

Quantitative analysis by LA-ICP-MS is affected by less easily manageable matrix interferences and laser instabilities and other non-quantifiable problems. Davies et al. [63] describe a comparative study of quantitative μ-XRF and LA-ICP-MS of Fe, Cu, and Zn in adjacent sections of murine neurological tissue. **Figure 4** shows representative examples of μ-XRF imaging of tissue sections showing the anatomical location of sectioned material and representative area of the coronal section analyzed by μ-XRF (dashed red box, 13 keV 2×7 μm^2 rectangular beam scanned over 500 μm × 500 μm) and LA-ICP-MS (dashed black box, considerably larger, 2.4 mm × 2.8 mm). The photomicrograph shows the substantia nigra pars compacta (SNc) neurons bordered by the midbrain reticular nucleus **(**MRN) and substantia nigra pars reticulata (SNr) tissue, corresponding to the region scanned by XRM. To the right in (c) Fe, Cu, and Zn X-ray images corresponding to the immune-stained SNc region. **Table 1** summarizes the quantitative results obtained. They suggest that LA-ICP-MS imaging is able to provide quantitative results that are comparable to those derived with μ-XRF.

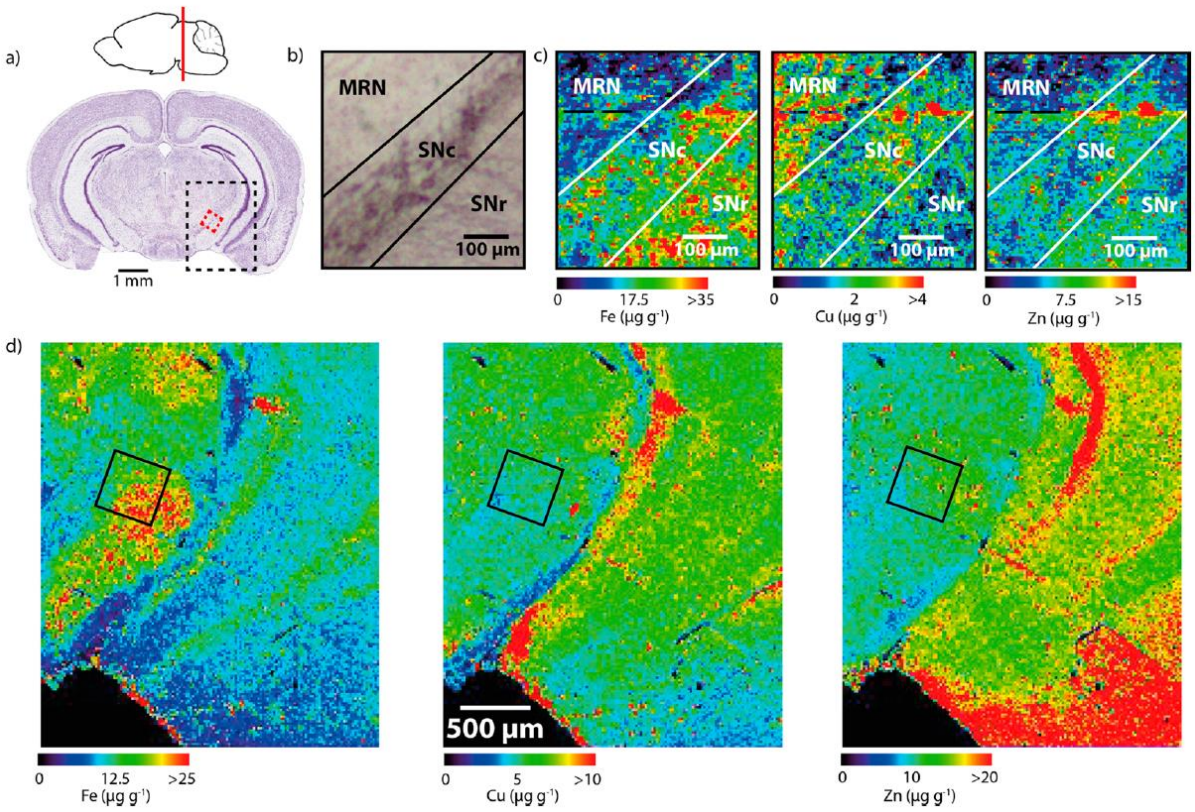

Figure 4: Representative examples of XRF images in brain tissue sections, false color imaging, see text. (a) Anatomical location of sectioned series; (b) Photomicrograph of tyrosine hydroxylase-positive SNc neurons bordered by MRN and SNr tissue; (c) XRM images of dashed red box; (d) LA-ICP-MS images of dashed black box. Reprinted with permission from K.M. Davies et al. [63]. Copyright 2015 American Chemical Society.

	Midbrain reticular nucleus			**Substantia nigra pars compacta**			**Substantia nigra pars reticulata**		
	Cu	**Fe**	**Zn**	**Cu**	**Fe**	**Zn**	**Cu**	**Fe**	**Zn**
XRF	3.86 ± 0.33	33.5 ± 12.8	18.5 ± 2.0	3.16 ± 0.10	35.4 ± 6.9	18.5 ± 0.7	3.19 ± 0.07	45.3 ± 14.0	19.5 ± 0.7
LA-ICP-MS	5.35 ± 0.36	23.8 ± 6.7	12.5 ± 0.8	5.20 ± 0.27	27.7 ± 6.0	13.6 ± 0.7	5.23 ± 0.18	33.8 ± 3.7	14.8 ± 0.9

Table 1: Regional Cu, Fe and Zn concentrations of MRN, SNc, and SNr brain regions as measured using XRF and LA-ICP-MS; all values are mean ± standard error of the mean in µg g^{-1}. Adapted with permission from K.M. Davies et al. [63]. Copyright 2015 American Chemical Society.

The interpretation of elemental images is affected by topological artefacts. These are most troublesome for the low energy fluorescence radiation of low atomic number elements due to the limited travel distances of low energy XRF emission and for inhomogeneities and mass density variations with dimensions comparable to the beam size. Artefacts and correction methods are reviewed by Billé et al. [97].

4.4 X-ray absorption spectroscopy

Inner-shell excitation by electrons or X-ray photons gives rise to ionization edges at energies equal to the inner-shell binding energies. The fine structure of X-ray absorption edges depends on the local chemical environment and the state of the excited atom. In atoms that are present in a specific chemical environment, the ionization edges are not sharply defined but are modulated by a fine structure that can be analyzed in terms of the electronic and atomic structure of the specimen, the X-ray absorption fine structure. Specific measurements of the absorption edge are commonly referred to as X-ray absorption spectroscopy (XAS). XAS can be exploited in X-ray absorption near edge structure (XANES), mainly as a fingerprinting tool. The destructive and constructive interference effects are used in extended X-ray absorption fine structure (EXAFS) in a more rigorous methodology that provides information on coordination number and distances to neighboring atoms, although in practice the heterogeneity of local environments for metals in brain tissue, and the low signal to noise, means that full EXAFS analysis is rarely possible unless the material of interest has been concentrated and/or purified. XANES and EXAFS information in each pixel can be acquired, in principle, by illuminating the sample with X-rays and by sweeping their energy across a core level of interest. In practice, one or more measurements below and above the absorption edge are used. Elemental speciation analysis through K or L edge energy scanning is now possible at micron or even sub-micron resolution. As mentioned in section 2, XANES provides opportunities to map different oxidation states in biological systems, including iron in neurodegenerative disorders (reviewed previously [15]) and sulfur in brain tumor tissue [21]. X-ray fluorescence at the sulfur K-edge recently also made it possible to image with chemical specificity for the sulfonate group of taurine in central nervous system sections [98]. This example illustrates how chemically-specific imaging for other sulfur species might be undertaken, such as sulfate esters which are abundant in white matter, and thiols and disulfides as important markers of oxidative stress and thiol redox [99].

Micro-XAS has proven useful in various fields of research such as metal-related neurodegeneration, scanning around the absorption edge of a specific metal [15], cellular pharmacology, trace element physiology, and metal toxicology. In biology, μ-XAS presents unique capabilities if compared to other speciation methods because it can be performed in situ, directly in subcellular compartments, without resorting to cell fractionation or other processing of the tissues which could extensively modify the chemical element species [75, 100].

4.5 Phase contrast imaging

Imaging contrast depends on the spatial variation of the refractive index within the sample. The absorption contrast mostly reflects the concentration of heavy metal stains in this case, since the organic material is quasi-transparent for hard X-rays. From the absorption, we can calculate the average attenuation factor that is proportional to the sample thickness.

Phase-gradient images describe the phase change of the emerging wavefront in the two orthogonal directions. They are very sensitive to thickness and compositional variations within the sample. Thus, they enhance the contrast of small features. The quantitative measurements of both absorption and phase give additional information about the sample. Because the real decrement of the refractive index (δ in the complex refractive index equation n = 1 - δ + i β), is much larger than the imaginary component (β), the phase-contrast usually is higher than the absorption-contrast [101]. The phase image is obtained by integrating the phase gradients afterwards. Imaging contrast can be made element-specific by tuning the energy around an absorption edge, where both δ and β vary rapidly. Phase-contrast X-ray images can also be acquired in an approach called coherent diffraction imaging (CDI) with a resolution beyond X-ray lens limits by recording the diffraction pattern from a coherently illuminated, non-crystalline sample [102].

Ptychography is a CDI based imaging technique, in which the electron density of the scattering material is determined from a series of two-dimensional scattering patterns via iterative reconstruction algorithms and redundant information from overlapping scanning positions. In theory, the spatial resolution of ptychography can reach the wavelength limit; in practice 3-nm resolution has been achieved when imaging silver nanocubes [103]. Simultaneous X-ray nano-ptychographic and fluorescence microscopy are combined in the Bionanoprobe at the APS. At this beamline biological samples can be directly observed in the frozen-hydrated state [56, 104].

4.6 X-ray tomography

Tomographic techniques, such as XRF-CT, are a 3D extension of the 2D XRF method. CT measurements are similar to conventional hospital CT scans but on a small scale, with massively increased resolution and with the added potential to obtain internal morphology, microstructure, and also compositional information. XRF-CT is obtained by recording a series of elemental images at different angular positions of the sample, rotating around an axis perpendicular to the beam. The resulting patterns (sinograms) are then subjected to mathematical procedures to produce an image of the radiation in the plane defined by the detector and the beam. By repeating this type of measurements on different planes while moving the sample the 3D image can eventually be generated.

The essential difference of XRF-CT from conventional CT is that the measurement is not based on the absorption of X–rays but on the measurement of the fluorescent X–rays with the ultimate aim of reconstructing compositional rather than density variations. This leads to a 3D dataset with a full X–ray spectrum, representative of the elemental composition for each constituent voxel. Recent developments in synchrotron beamline technology (including the Maia detector offering rapid acquisition of XRF spectra at the Australian Synchrotron XFM beamline [105]), and advanced sample preparation and manipulation [106], are significantly advancing XRF-CT in biological specimens [107].

It is also possible to obtain local analytical information from inside a specimen by XRF confocal scanning (which uses a 90° fluorescence configuration distinct from that used in visible light confocal microscopy)**.** Here the measurements rely on X–ray lenses that focus incoming and outgoing radiation inside the specimen, thus enabling the direct elemental analysis of specific locations in the beam path below the sample. This method provides a suitable alternative to XRF-CT for the detailed analysis of specific inclusions in larger samples. It allows one to map a specific predetermined microscopic ROI with high lateral resolution, and by systematic measurement over three spatial dimensions it provides 3D analysis in a more direct way than XRF-CT [108]. XRF-CT can be performed while scanning around particular absorption edges to provide 3D XAS data. X-ray phase contrast CT (PC-CT) relies on the phase shift that X-rays undergo when passing through matter. It developed into a powerful set of tools for soft tissues and low atomic number samples and discloses sample features that cannot be practically imaged using absorption contrast. Such phase derived contrast is often several orders of magnitude stronger than the absorption contrast, thus allowing the reduction of exposure times and lowering sample irradiation doses.

Micro–CT is also available in a range of easy–to–use desktop instruments. Several laboratory microtomographs have been commercially produced over the last years. Laboratory X–Ray absorption CT operates routinely to voxel dimensions of one cubic µm, while SR–based CT facilities have achieved a spatial resolution of the order of tens of nm. While SR X-ray sources are needed for sub-microscopic spatial resolution imaging at the cellular level and below, bench-top instruments can be used for coarser scans of the sample to identify ROIs for detailed imaging purposes.

4.7 Nano beamlines

The methods considered up to this point in the chapter are based on hard X-rays, and can generally be subdivided into two modalities: techniques which focus on the chemical composition (XRF and XAS), and techniques which focus on the structural or morphological information with X-ray CT (e.g., absorption or phase CT). Both aspects are equally important: for biological imaging of metals in brain tissue, a full morphological and chemical characterization is desired. For this reason, several synchrotron radiation facilities in the world have recently implemented beamlines to combine 3D XRF with transmission XCT, targeting nanoscopic-resolution levels. A world-leading example of this integrated approach is represented by the new Nano-Imaging Nano-Analysis (NINA) facility at the ESRF, which provides the most intense hard X-ray nanobeam in the world, aiming at a spatial resolution level of 10 nm for hard X-rays as part of a major upgrade of the source between 2015-2022 [109]. Hard X-ray nano-beam imaging is also available at other synchrotrons including the established APS beamline 2-ID-D, and the Diamond Light Source beamline I14 which will become operational from 2017.

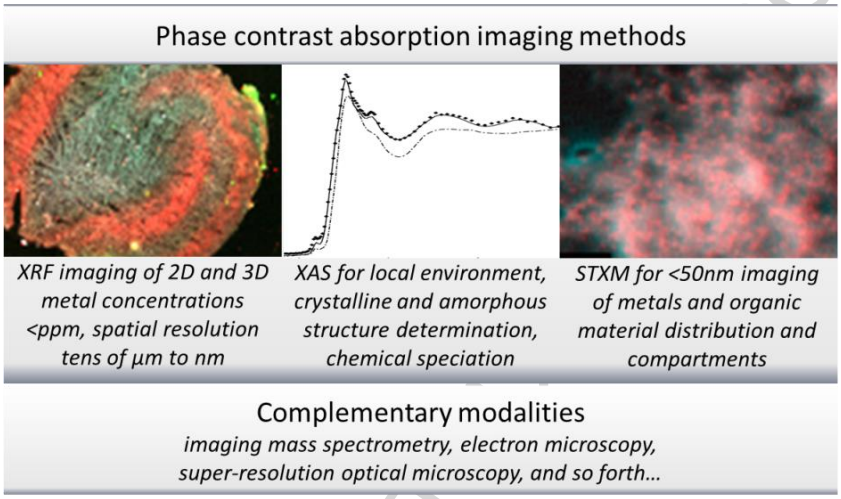

Figure 5: Multi-keV microscopy approaches in neurometallobiology, providing metal concentrations and element distributions, chemical state (speciation), mineral phase or other compound where relevant, and co-localization with specific structures or compartments at subcellular resolutions.

Figure 5 summarizes how several tools of an X-ray microspectroscopy beamline can provide insight into the three key aspects (distribution, concentration, speciation) when dealing with metallobiology of the brain [68]. The role of metals in the brain and the central nervous system relies on the 2D and 3D imaging of metals at multiple length scales from the nanoscopic and sub-microscopic level to the macroscopic and its correlation with a number of other imaging techniques and XRM observational tools provided by phase contrast imaging methods.

4.8 X-ray diffraction

When XRD (X-ray diffraction) signals are detected by using a 2D detector, a crystalline phase distribution image is obtained [110]. When XRF, XAS, and XRD signals are collected from a sample simultaneously, a detailed understanding of the chemical species and structures of materials in the sample can be developed [102]. Sub-cellular structure and nanometer-sized cell components can be revealed with X-ray probes within intact biological cells by measuring the distribution of density

contrast as obtained by phase reconstruction schemes, thus assisting in the interpretation of the metal imaging data [68]. Scanning X-ray nanodiffraction can be employed to record reciprocal space scattering patterns from ROIs in elemental imaging. A combination of ptychography and scanning X-ray nanodiffraction can be used to reveal the internal structural arrangement and diameter of keratin bundles in whole cells [111].

The great depth of penetration of X-rays in matter allows the investigation of the interior of objects without destructive sample preparation or sectioning. X-rays can penetrate through a thick sample, e.g. at 12 keV, the penetration depth for biological samples is over 3 mm. This implies for XRF imaging that the detected analytical information represents the full line–integral along the path where the micro–beam penetrates the sample. A typical scanning µ-XRF experiment therefore results in a 2D projection of the elemental distributions within the examined sample, without any significant depth information. Since structures end up superimposed in the image, such projection images are difficult to interpret, and it is beneficial therefore to prepare sections for imaging which are the thickness of the feature (for example, a particular cell type) of interest. For microfocus-resolution XRF imaging (section 4.2) and XANES measurements (section 4.4) with a hard X-ray beam, cryosections of brain tissue with thickness ~ 10 µm typically provide sufficient material to obtain good signal-to-noise for efficient imaging of the transition metals most abundant in the tissue (iron, zinc, copper) and scope to detect elements normally present at lower concentrations (e.g. manganese). These sections also provide sufficient signal from locally elevated concentrations to obtain XANES spectra that can be fitted with standards to determine chemical valence and in many instances also to identify the dominant forms of metal ion storage (e.g. ferrihydrite-like mineral cores in ferritin) [15, 112]. Significantly thinner sections (typically 500 nm) can be prepared for nanobeam analysis while retaining sufficient material to obtain useful spectra for chemical imaging and characterization of the main transition metals.

4.9 Soft X-ray imaging

Soft X-rays penetrate hydrated specimens more deeply than electrons do, and produce bright-field images with much higher resolution than is possible using visible light. Soft X-ray microscopy at a lower energy (~0.1 - 1 keV) has a unique spectral region termed the 'water window', situated between the carbon and oxygen K–absorption edges at 284 and 540 eV, where soft X-rays are strongly absorbed by carbon–rich biological structures while attenuation by surrounding oxygen–dominated material (ice) is minimal. Thus, frozen hydrated biological specimens can be imaged at around 500 eV without the need for additional contrast agents. An additional and significant advantage of imaging biological samples with soft X–rays is that the latter still have sufficient energy to achieve a penetration depth of about 10 µm. As a consequence, soft X-ray microscopes can view most biological cells intact. Cryo-Soft X-ray Tomography (cryo-SXT) is unique in its ability to image intact cells without the need to section them [113, 114]. SXT has now been applied to imaging a wide range of different cell types, ranging in size from small bacteria to mammalian cells derived from living tissue. Among high-resolution structure imaging methods SXT has the unique capacity to image the nucleus in intact mammalian cells [6].

In scanning transmission X-ray microscopy (STXM) an X-ray beam is focused down to a sub-micron diameter spot, typically to scan a sample in the focal plane and record the transmitted X-ray intensity as a function of the sample position. As such, it is similar in design to the conventional light microscope and the scanning transmission electron microscope (STEM). Typical focal points (and thereby spatial resolutions) are of the order of 15-50 nm in diameter. STXM is usually used in the soft X-ray range for biological applications where it has the advantage over TEM that the biological samples can be observed in their natural state and that radiation damage is reduced by orders of

magnitude. When applied with variable X-ray energy the method provides absorption spectra similar to those obtained with energy-filtering TEM. By measuring the specimen transmission at different photon energies, STXMs can provide quantitative information on the specimen's local elemental and chemical composition on nm-size areas [77]. An example is given in **Figure 6**. Where the sections are too thick to image at the carbon K-edge (as in **Figure 6 A**), the protein absorption feature at the oxygen K-edge is used to obtain an image of protein density distribution. The amount of material in thicker sections (~ 500 nm) has the simple advantage of permitting better observation of tissue structure than the thinner sections (typically 100 -200 nm). The thinner sections (as in **Figure 6 B**) permit inclusion of the carbon K-edge, so that protein and carbonate distribution can be imaged. Note that the oxygen K-edge energy for the carbonate distribution mapping is slightly offset from the energy used to obtain the protein maps (part **A**), as it corresponds to a carbonate-specific feature in the spectrum. Careful utilization of features in edge-energy spectra therefore allows specific identification of multiple organic and inorganic compounds in a single section, making this a very powerful technique. The method is now available in many SR facilities, including an outstanding example at the ALS Beamline 11.0.2, and the recently commissioned STXM beamline I08 at Diamond Light Source.

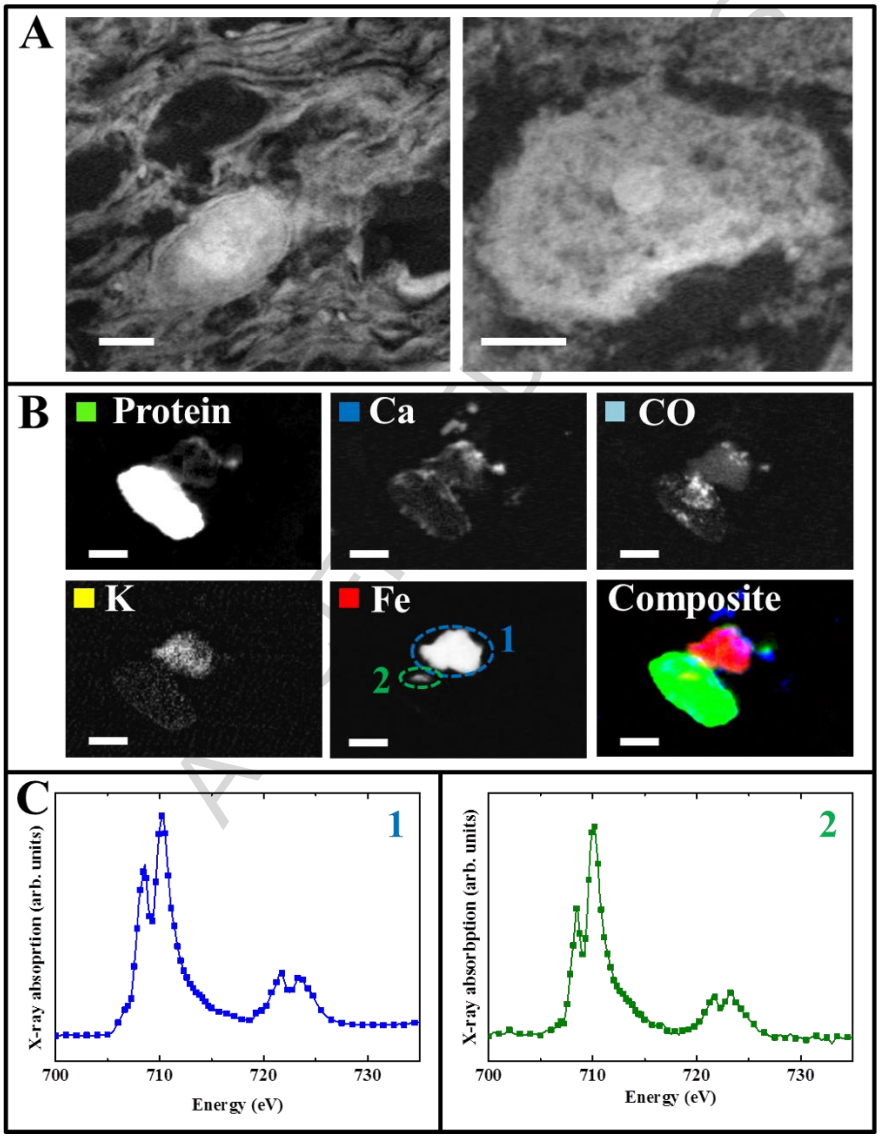

Figure 6: **A)** Oxygen K-edge speciation maps showing tissue structure in resin-embedded human putamen (left) and amygdala (right). X-ray beam acquisition energy: 532.1 eV. [Scale bars = 2µm]. **B)** Speciation maps of a protein deposit in human AD plaque-rich amygdala tissue. Maps were acquired at the carbon K-edge (285.2 eV; protein), calcium L-edge (352.6 eV), oxygen K-edge (carbonate; 533.8 eV), potassium L-edge (300 eV) and iron L-edge (710 eV). The composite image uses the colors indicated in the individual map panels. [Scale bars = 2µm]. **C)** Iron $L_{2,3}$-edge absorption spectra taken from the iron deposits identified in the Fe contrast map in part B. Image provided courtesy of J. Everett, V.T. Tjhin, J.F. Collingwood, and N.D. Telling, using data obtained at the ALS beamline 11.0.2, and human tissue provided by L.N. Hazrati on behalf of the Canadian Brain Tissue Bank under UK ethical approval 07-MRE08-12.

5. X-ray imaging correlated with other imaging methods

Biochemical processes, including those that take place in the brain, are based on the interactions between various molecules and molecular complexes, and their dynamic spatial redistribution. Despite their multi-modal possibilities, X-ray microscopes that measure the detailed distribution in cellular material are only part of the analytical tools necessary to understand these complicated biochemical interactions. In particular, it is necessary to identify the molecular entities involved and to determine their spatial distribution. The analytical tools that are used to study these processes should provide as much information as possible about the identities and topographical distributions of the chemical species present within biological samples. Complementary information becomes available by combining imaging techniques that use different physical principles and, therefore, produce images representing different properties of the sample. The modern synchrotron X-ray microscopes can be differentiated by individualized combinations of analytical and observational tools optimized to study particular systems.

Metal distributions in brain tissue slices which can be combined with conventional imaging modalities such as photomicrography of native or processed tissue such as histochemistry or immunostaining), autoradiography or with in vivo functional imaging techniques such as positron emission tomography or magnetic resonance tomography. MSI is a powerful tool for directly determining the distribution of proteins, peptides, lipids, neurotransmitters, metabolites and drugs in neural tissue sections in situ [115]. Correlative imaging of metals with XRM and various organic compounds with MSI techniques, such as matrix assisted laser desorption (MALDI) or SIMS, provides an insight into the presence and the behavior of metal containing compounds in the cellular structures. It is possible to correlate fluorescence images and X-ray tomograms of frozen-hydrated cells, providing whole cell analysis with all the advantages of fluorescence detection in addition to sub-30 nm resolution. In work to better describe the role of neuromelanin in regulating metal elements within neurons, metal accumulation (with the spatial distribution of the individual elements determined by XRF at 80 nm resolution) has been co-localized to neuromelanin pigment evaluated by optical microscopy in dopaminergic neurons of the substantia nigra [26].

The combination of images from two or more such complementary modalities produces significantly greater insights than is possible using the X-ray microscopes alone. Landmarks, such as patterns of cells, irregularities in section edges, or deliberately-introduced features clearly visible in data from both modalities, are used to accurately overlay data sets onto the other to produce a 2D or 3D multi-modal reconstruction. Image manipulation to achieve this may be undertaken using a number of open-source tools, and many laboratories undertake the correction by hand if the number of images involved is small, or use macros developed in-house.

Recent studies show examples of the power of combining a suite of complementary imaging techniques. For example, Que et al. [116] achieved zinc imaging in live cells with the use of a chemical fluorescent probe, XRM with 3D elemental tomography, STEM and energy-dispersive spectroscopy (EDS) with a histochemical staining protocol. In this study it was established that 'zinc sparks', which are essential for the egg-to- embryo transition, originate from a system of thousands of vesicles, each of which contains approximately 10^6 zinc atoms [116]. Meanwhile, Kashiv et al. [117] mapped elemental distributions, including trace metals, for single organelles and other subcellular features using XRF at 40 nm resolution following initial characterization by TEM.

6. Practical aspects

This review has provided an overview of XRM methods as they have developed. It encapsulates X-ray microscopy to detect metals in the brain on length scales from whole brain sections down to the cellular and sub-cellular level. The large penetration depth of hard X-rays, ranging from microns to millimeters in a biological matrix, offers possibilities for simple sample preparation procedures and more versatile in situ observations in controlled environments. There is no default requirement for vacuum conditions, and experiments can be performed on frozen/hydrated samples, thus reducing radiation damage and optimizing the preservation of cell structure.

Concerning the sample preparation, there are principles to be understood but there is no universally applicable procedure, the sample treatment steps being primarily determined by the biological specimen itself. Each biological sample requires careful optimization and testing of the preparation procedure to minimize artefacts. When performing chemical elemental imaging within biological structures, SR-based scanning techniques require that the properties of interest in the biological sample remain unchanged during the time frame of the measurement, which may be up to several hours, during which 2D raster scans are performed by moving the sample through the X-ray beam. In order to be able to perform such analysis on the nanoscopic level, the definition of the focal point for the X-ray beam, the immobilization of the sample on the motor stage system and the accurate and precise movements of the sample to preserve the sample position relative to the focal point, are real challenges. It is important to consider whether the hydration state of the original material will be preserved, e.g. by analysing the sample under cryogenic conditions, or whether the sample will necessarily be dehydrated. Exposure of a hydrated sample to a micro or nano-focussed SR X-ray beam at room temperature can significantly compromise the experiment, causing irreversible damage including rapid displacement of material within the sample matrix. The consequence of dehydration for the species under investigation needs to be evaluated, along with the impact of sample preparation and X-ray exposure on the viability of subsequent histological analysis of the sample. In some cases, simple staining that confirms the location of cells in a tissue section is sufficient, but requirements are inevitably study-dependent and it may be necessary to utilize appropriately preserved adjacent sections to correlate information about metals with tissue structure. Depending on the metal, working with chemically fixed or resin-embedded samples (as opposed to fresh or frozen) may ensure the metal species of interest are retained, or result in their unintended mobilization [54, 55]. The impact of sample archiving and handling on the distribution and concentration of trace elements in the sample, on length scales relevant to the experiment design, needs full consideration.

Practical aspects of sample preparation, handling, data collection, 3D reconstruction, structure analysis and sample contrasting methods for hard X-ray tomography are approached in detail in the review of Mizutani and Suzuki [118]. Specific advances are detailed elsewhere in the literature: Perrin et al report a study was to develop and validate a standard protocol for single-cell quantitative

imaging of the elements using SR XRF [119]. Their results suggest that the optimal sample preparation method to study elemental distribution in single whole cells prepared for X-ray microanalysis is achieved when cells are rinsed with ammonium acetate, quickly frozen by plunging into liquid nitrogen–chilled cryogenic fluid and freeze-dried at low temperatures. This protocol was also successfully validated on rat primary hippocampal neurons, a delicate in vitro neuronal model.

Substrates to support the sample have the disadvantage that they limit beam transmission and give rise to scattering of radiation. As ultra-thin membranes for sample support, two-dimensional materials such as graphene, molybdenum disulphide and boron nitride have been considered. Of special interest are silicon nitride (Si_3N_4) membranes which can be fabricated with well-defined density, thickness down to less than 3 nm and perfect homogeneity [120]. Silicon nitride membranes are a versatile sample support, particularly for work with cultured cells that do not contain Si, and they facilitate multi-modal imaging ranging from the hard X-ray region to the infrared [121]. In vivo 2D and 3D elemental imaging of free-standing biological microorganisms or single cells, present in their aqueous environment, is now possible. Under ideal conditions, a delicate biological sample would not be dependent on a sample support. To achieve this, optical tweezers are being introduced for positioning and manipulating an observing the sample while keeping it in its natural state [122]. This offers new opportunities for XRM analyses of metals in neurological materials.

The majority of synchrotrons operate a competitive peer-reviewed application process to allocate beamtime, with a proportion set aside for paid access by industrial users, or for collaborations of users who have made a significant investment in the beamline, for example. There is a large demand for beam time and it is thus imperative to present a good proposal with clearly defined research objectives. Synchrotrons run 24 hours day and night to provide high intensity light beams to accommodate a maximum number of research groups. The high cost of operating synchrotron facilities means that even if the allocation is free at point of use for the successful applicant, it is important to make the best possible use of the allocated time, balancing factors such as spatial resolution and dwell time to optimise measurement efficiency, and utilizing the delivered beam day and night throughout the experiment period [123].

7. Conclusion

Progress of the sciences depends on new concepts (theories; knowledge and concept driven) and new tools (instrumentation, technological advances; data-driven). Dyson states that tool-driven concepts are decisive in the recent development of most sciences, particularly in fields such as biology and astronomy [124]. As quoted by the EuroScience Open Forum [125]:

"*Nature and the Universe are at their most thrilling when revealed at their largest, smallest and fastest scales. Instrumental techniques are now available to describe the composition, the structure and the function of the smallest dimensions of materials and matter, the fastest chemical processes, and the most extreme and challenging cellular, terrestrial and extra-terrestrial environments*".

Meanwhile Kitchin [126] states that: "*Data driven science challenges the established scientific deductive approach, it allows us to discover, inductively, new things that then need to be explained".*

In summary: "*New truths become evident when new tools become available"*. With this quote from Rosalyn Sussman Yarow, 1977 Nobel Prize in Physiology and Medicine, she underlines the importance of new observational tools to provide answers to scientific questions, and to allow the formulation of new questions.

Developments in observational tools, including new "visualization" analytical instrumentation, are critical for a new conceptual framework in analytical chemistry and transfer the discipline into the

realms of data-driven science. Among these, X-ray microscopy is a significant new tool for the detailed investigation and study of the heterogeneous structure and composition of natural and man-made materials. With its different interaction mechanisms, XRM is considered the “Swiss Army knife”, the leading multi-faceted tool among the methods for microscopic and nanoscopic imaging analysis. For biological materials it meets the criteria of complementing data from existing modalities while providing totally unique views of cells and tissues. In particular, XRM allows the quantitative imaging of numerous elements and elemental compounds within intact biological cells down to the level of nanometer-sized objects and structures. The combination of the superior penetration power of X-rays, and their high sensitivity for quantitative elemental analysis at high spatial resolution, creates a unique tool with capabilities that other microscopy techniques based on electron or light microscopy cannot provide. While X-ray techniques need SR sources for optimum performance, they can also be implemented with micro-focus laboratory sources at reduced spatial resolution and sensitivity. In addition, SR μ-XRF is quantitative, providing a unique opportunity to non-destructively quantify and localize metals in-situ in individual cultured cells [66]. With SR XRMs, elemental imaging of biological materials is possible with sub-cellular spatial resolution, at the level of the organelle. The combination of high spatial resolution and sensitivity is unmatched by any other elemental imaging technique. It is possible to obtain absorption-, phase-, and fluorescence-contrast images of unstained biological samples at different levels of magnification ranging from the nano-size sub-cellular functional units to the macroscopic level of the organ. The nanometer spatial resolution of the microscope, and its diverse imaging modalities, enables hyper-spectral observation of metal composition throughout the morphological ultra-structure of comparatively thick biological samples in their native state.

8. Acknowledgements

This work was supported in part by the EPSRC [EP/K035193/1], and through beamtime allocations at the Diamond Light Source [beamline I18] and the Advanced Light Source [beamline 11.0.2]. The Advanced Light Source is supported by the Director, Office of Science, Office of Basic Energy Sciences, of the U.S. Department of Energy under Contract No. DE-AC02-05CH11231. Selected parts of this paper are adapted from the chapter ‘X-ray microscopy for detection of metals in the brain’ to be published in the Springer NEUROMETHODS volume ‘Metals in the Brain: Measurement and Imaging’ [127].

9. References

[1] E.L. Que, D.W. Domaille, C.J. Chang, Metals in neurobiology: probing their chemistry and biology with molecular imaging, Chemical reviews, 108 (2008) 1517-1549.
[2] N. Principi, S. Esposito, Gut microbiota and central nervous system development, The Journal of infection, 73 (2016) 536-546.
[3] F.W. Outten, B.S. Twining, Metal Homeostasis, John Wiley & Sons, 2008.
[4] C.J. Chang, Searching for harmony in transition-metal signaling, Nature chemical biology, 11 (2015) 744-747.
[5] R. Lobinski, J.S. Becker, H. Haraguchi, B. Sarkar, Metallomics: Guidelines for terminology and critical evaluation of analytical chemistry approaches (IUPAC Technical Report), Pure and Applied Chemistry, 82 (2010) 493-504.
[6] M. Do, S.A. Isaacson, G. McDermott, M.A. Le Gros, C.A. Larabell, Imaging and characterizing cells using tomography, Archives of biochemistry and biophysics, 581 (2015) 111-121.
[7] D.Y. Parkinson, L.R. Epperly, G. McDermott, M.A. Le Gros, R.M. Boudreau, C.A. Larabell, Nanoimaging cells using soft X-ray tomography, Methods in molecular biology (Clifton, N.J.), 950 (2013) 457-481.

[8] S. Habuchi, Super-resolution molecular and functional imaging of nanoscale architectures in life and materials science, Frontiers in bioengineering and biotechnology, 2 (2014) 20.
[9] D. Vanhecke, S. Asano, Z. Kochovski, R. Fernandez-Busnadiego, N. Schrod, W. Baumeister, V. Lucic, Cryo-electron tomography: methodology, developments and biological applications, Journal of microscopy, 242 (2011) 221-227.
[10] E. Nakazawa, T. Ikemoto, A. Hokura, Y. Terada, T. Kunito, S. Tanabe, I. Nakai, The presence of mercury selenide in various tissues of the striped dolphin: evidence from mu-XRF-XRD and XAFS analyses, Metallomics : integrated biometal science, 3 (2011) 719-725.
[11] M. Korbas, J.L. O'Donoghue, G.E. Watson, I.J. Pickering, S.P. Singh, G.J. Myers, T.W. Clarkson, G.N. George, The chemical nature of mercury in human brain following poisoning or environmental exposure, ACS chemical neuroscience, 1 (2010) 810-818.
[12] T. Bacquart, G. Deves, A. Carmona, R. Tucoulou, S. Bohic, R. Ortega, Subcellular speciation analysis of trace element oxidation states using synchrotron radiation micro-X-ray absorption near-edge structure, Analytical chemistry, 79 (2007) 7353-7359.
[13] R. Ortega, P. Cloetens, G. Deves, A. Carmona, S. Bohic, Iron storage within dopamine neurovesicles revealed by chemical nano-imaging, PloS one, 2 (2007) e925.
[14] M.J. Keogh, C.M. Morris, P.F. Chinnery, Neuroferritinopathy, International review of neurobiology, 110 (2013) 91-123.
[15] J.F. Collingwood, M.R. Davidson, The role of iron in neurodegenerative disorders: insights and opportunities with synchrotron light, Frontiers in pharmacology, 5 (2014) 191.
[16] R. McRae, P. Bagchi, S. Sumalekshmy, C.J. Fahrni, In situ imaging of metals in cells and tissues, Chemical reviews, 109 (2009) 4780-4827.
[17] W. Maret, The Metals in the Biological Periodic System of the Elements: Concepts and Conjectures, International journal of molecular sciences, 17 (2016) 66-72.
[18] A.H. Tang, H. Chen, T.P. Li, S.R. Metzbower, H.D. MacGillavry, T.A. Blanpied, A trans-synaptic nanocolumn aligns neurotransmitter release to receptors, Nature, 536 (2016) 210-214.
[19] F. Adams, C. Barbante, Spectroscopic Imaging, in: Comprehensive Analytical Chemistry, Elsevier Science Ltd., 2015, pp. 340-376.
[20] A.S. McCall, C.F. Cummings, G. Bhave, R. Vanacore, A. Page-McCaw, B.G. Hudson, Bromine is an essential trace element for assembly of collagen IV scaffolds in tissue development and architecture, Cell, 157 (2014) 1380-1392.
[21] M. Szczerbowska-Boruchowska, Z. Stegowski, M. Lankosz, M. Szpak, D. Adamek, A synchrotron radiation micro-X-ray absorption near edge structure study of sulfur speciation in human brain tumors—a methodological approach, J. Anal. At. Spectrom., 27 (2012) 239-247.
[22] J.I. Toohey, A.J. Cooper, Thiosulfoxide (sulfane) sulfur: new chemistry and new regulatory roles in biology, Molecules, 19 (2014) 12789-12813.
[23] M. Kuhbacher, J. Bartel, B. Hoppe, D. Alber, G. Bukalis, A.U. Brauer, D. Behne, A. Kyriakopoulos, The brain selenoproteome: priorities in the hierarchy and different levels of selenium homeostasis in the brain of selenium-deficient rats, Journal of neurochemistry, 110 (2009) 133-142.
[24] N.D. Solovyev, Importance of selenium and selenoprotein for brain function: From antioxidant protection to neuronal signalling, Journal of inorganic biochemistry, 153 (2015) 1-12.
[25] K.J. Barnham, A.I. Bush, Biological metals and metal-targeting compounds in major neurodegenerative diseases, Chemical Society reviews, 43 (2014) 6727-6749.
[26] S. Bohic, K. Murphy, W. Paulus, P. Cloetens, M. Salome, J. Susini, K. Double, Intracellular chemical imaging of the developmental phases of human neuromelanin using synchrotron X-ray microspectroscopy, Analytical chemistry, 80 (2008) 9557-9566.
[27] T. Skjorringe, L.B. Moller, T. Moos, Impairment of interrelated iron- and copper homeostatic mechanisms in brain contributes to the pathogenesis of neurodegenerative disorders, Frontiers in pharmacology, 3 (2012) 169.
[28] M.A. Greenough, A. Ramirez Munoz, A.I. Bush, C.M. Opazo, Metallo-pathways to Alzheimer's disease: lessons from genetic disorders of copper trafficking, Metallomics : integrated biometal science, 8 (2016) 831-839.

[29] A. Sigel, H. Sigel, R.K.O. Sigel, Metallothioneins and related chelators, RSC Publishing, 2009.
[30] K.M. Dean, Y. Qin, A.E. Palmer, Visualizing metal ions in cells: an overview of analytical techniques, approaches, and probes, Biochimica et biophysica acta, 1823 (2012) 1406-1415.
[31] S. Yamasaki, K. Sakata-Sogawa, A. Hasegawa, T. Suzuki, K. Kabu, E. Sato, T. Kurosaki, S. Yamashita, M. Tokunaga, K. Nishida, T. Hirano, Zinc is a novel intracellular second messenger, The Journal of cell biology, 177 (2007) 637-645.
[32] C.N. Waters, J. Zalasiewicz, C. Summerhayes, A.D. Barnosky, C. Poirier, A. Galuszka, A. Cearreta, M. Edgeworth, E.C. Ellis, M. Ellis, C. Jeandel, R. Leinfelder, J.R. McNeill, D. Richter, W. Steffen, J. Syvitski, D. Vidas, M. Wagreich, M. Williams, A. Zhisheng, J. Grinevald, E. Odada, N. Oreskes, A.P. Wolfe, The Anthropocene is functionally and stratigraphically distinct from the Holocene, Science, 351 (2016) aad2622.
[33] A. Cvetkovic, A.L. Menon, M.P. Thorgersen, J.W. Scott, F.L. Poole, 2nd, F.E. Jenney, Jr., W.A. Lancaster, J.L. Praissman, S. Shanmukh, B.J. Vaccaro, S.A. Trauger, E. Kalisiak, J.V. Apon, G. Siuzdak, S.M. Yannone, J.A. Tainer, M.W. Adams, Microbial metalloproteomes are largely uncharacterized, Nature, 466 (2010) 779-782.
[34] C.M. Gionfriddo, M.T. Tate, R.R. Wick, M.B. Schultz, A. Zemla, M.P. Thelen, R. Schofield, D.P. Krabbenhoft, K.E. Holt, J.W. Moreau, Microbial mercury methylation in Antarctic sea ice, Nature microbiology, 1 (2016) 16127.
[35] T.A. Rouault, Iron metabolism in the CNS: implications for neurodegenerative diseases, Nature reviews. Neuroscience, 14 (2013) 551-564.
[36] C. Exley, Why industry propaganda and political interference cannot disguise the inevitable role played by human exposure to aluminum in neurodegenerative diseases, including Alzheimer's disease, Frontiers in Neurology, 5 (2014) 1-6.
[37] K.M. Davies, S. Bohic, A. Carmona, R. Ortega, V. Cottam, D.J. Hare, J.P. Finberg, S. Reyes, G.M. Halliday, J.F. Mercer, K.L. Double, Copper pathology in vulnerable brain regions in Parkinson's disease, Neurobiology of aging, 35 (2014) 858-866.
[38] Y.H. Hung, A.I. Bush, R.A. Cherny, Copper in the brain and Alzheimer's disease, Journal of biological inorganic chemistry : JBIC : a publication of the Society of Biological Inorganic Chemistry, 15 (2010) 61-76.
[39] A.H. Koeppen, R.L. Ramirez, D. Yu, S.E. Collins, J. Qian, P.J. Parsons, K.X. Yang, Z. Chen, J.E. Mazurkiewicz, P.J. Feustel, Friedreich's ataxia causes redistribution of iron, copper, and zinc in the dentate nucleus, Cerebellum, 11 (2012) 845-860.
[40] M.W. Bourassa, L.M. Miller, Metal imaging in neurodegenerative diseases, Metallomics : integrated biometal science, 4 (2012) 721-738.
[41] R.A. Yokel, Blood-brain barrier flux of aluminum, manganese, iron and other metals suspected to contribute to metal-induced neurodegeneration, J Alzheimers Dis, 10 (2006) 223-253.
[42] E. House, J. Collingwood, A. Khan, O. Korchazkina, G. Berthon, C. Exley, Aluminium, iron, zinc and copper influence the in vitro formation of amyloid fibrils of Abeta42 in a manner which may have consequences for metal chelation therapy in Alzheimer's disease, J Alzheimers Dis, 6 (2004) 291-301.
[43] R.J. Ward, D.T. Dexter, R.R. Crichton, Neurodegenerative diseases and therapeutic strategies using iron chelators, Journal of trace elements in medicine and biology : organ of the Society for Minerals and Trace Elements, 31 (2015) 267-273.
[44] Y.-X. Wang, S. Xuan, M. Port, J.-M. Idee, Recent Advances in Superparamagnetic Iron Oxide Nanoparticles for Cellular Imaging and Targeted Therapy Research, Current Pharmaceutical Design, 19 (2013) 6575-6593.
[45] N. Scherf, J. Huisken, The smart and gentle microscope, Nat Biotech, 33 (2015) 815-818.
[46] J.A.G. Briggs, M. Lakadamyali, Imaging cellular structure across scales with correlated light, superresolution, and electron microscopy, Molecular Biology of the Cell, 23 (2012) 979-980.
[47] C. Loussert Fonta, B.M. Humbel, Correlative microscopy, Archives of biochemistry and biophysics, 581 (2015) 98-110.
[48] D.J. Hare, E.J. New, M.D. de Jonge, G. McColl, Imaging metals in biology: balancing sensitivity, selectivity and spatial resolution, Chemical Society reviews, 44 (2015) 5941-5958.

[49] B. Laforce, B. Vermeulen, J. Garrevoet, B. Vekemans, L.V. Hoorebeke, C. Janssen, L. Vincze, Laboratory Scale X-ray Fluorescence Tomography: Instrument Characterization and Application in Earth and Environmental Science, Analytical chemistry, 88 (2016) 3386-3391.
[50] K. Jurowski, B. Buszewski, W. Piekoszewski, Bioanalytics in Quantitive (Bio)imaging/Mapping of Metallic Elements in Biological Samples, Critical reviews in analytical chemistry, 45 (2015) 334-347.
[51] M. Bartels, M. Priebe, R.N. Wilke, S.P. Krüger, K. Giewekemeyer, S. Kalbfleisch, C. Olendrowitz, M. Sprung, T. Salditt, Low-dose three-dimensional hard x-ray imaging of bacterial cells, Optical Nanoscopy, 1 (2012) 10.
[52] H. Yan, E. Nazaretski, K. Lauer, X. Huang, U. Wagner, C. Rau, M. Yusuf, I. Robinson, S. Kalbfleisch, L. Li, N. Bouet, J. Zhou, R. Conley, Y.S. Chu, Multimodality hard-x-ray imaging of a chromosome with nanoscale spatial resolution, Scientific reports, 6 (2016) 20112.
[53] M.M. van Schooneveld, S. DeBeer, A close look at dose: Toward L-edge XAS spectral uniformity, dose quantification and prediction of metal ion photoreduction, Journal of Electron Spectroscopy and Related Phenomena, 198 (2015) 31-56.
[54] Q. Jin, T. Paunesku, B. Lai, S.C. Gleber, S.I. Chen, L. Finney, D. Vine, S. Vogt, G. Woloschak, C. Jacobsen, Preserving elemental content in adherent mammalian cells for analysis by synchrotron-based x-ray fluorescence microscopy, Journal of microscopy, 265 (2017) 81-93.
[55] S.A. James, D.E. Myers, M.D. de Jonge, S. Vogt, C.G. Ryan, B.A. Sexton, P. Hoobin, D. Paterson, D.L. Howard, S.C. Mayo, M. Altissimo, G.F. Moorhead, S.W. Wilkins, Quantitative comparison of preparation methodologies for X-ray fluorescence microscopy of brain tissue, Analytical and bioanalytical chemistry, 401 (2011) 853-864.
[56] S. Chen, J. Deng, Y. Yuan, C. Flachenecker, R. Mak, B. Hornberger, Q. Jin, D. Shu, B. Lai, J. Maser, C. Roehrig, T. Paunesku, S.C. Gleber, D.J. Vine, L. Finney, J. VonOsinski, M. Bolbat, I. Spink, Z. Chen, J. Steele, D. Trapp, J. Irwin, M. Feser, E. Snyder, K. Brister, C. Jacobsen, G. Woloschak, S. Vogt, The Bionanoprobe: hard X-ray fluorescence nanoprobe with cryogenic capabilities, Journal of synchrotron radiation, 21 (2014) 66-75.
[57] T. Paunesku, S. Vogt, J. Maser, B. Lai, G. Woloschak, X-ray fluorescence microprobe imaging in biology and medicine, Journal of cellular biochemistry, 99 (2006) 1489-1502.
[58] A.H. Zewail, Four-dimensional electron microscopy, Science, 328 (2010) 187-193.
[59] G.W. Grime, High-energy ion beam analysis, in: J. Reedjijk (Ed.) Reference Module in Chemistry, Molecular Sciences, and Chemical Engineering, Elsevier, 2014.
[60] S.G. Boxer, M.L. Kraft, P.K. Weber, Advances in imaging secondary ion mass spectrometry for biological samples, Annual review of biophysics, 38 (2009) 53-74.
[61] J.S. Becker, Imaging of metals in biological tissue by laser ablation inductively coupled plasma mass spectrometry (LA-ICP-MS): state of the art and future developments, Journal of mass spectrometry : JMS, 48 (2013) 255-268.
[62] H.A. Wang, D. Grolimund, C. Giesen, C.N. Borca, J.R. Shaw-Stewart, B. Bodenmiller, D. Gunther, Fast chemical imaging at high spatial resolution by laser ablation inductively coupled plasma mass spectrometry, Analytical chemistry, 85 (2013) 10107-10116.
[63] K.M. Davies, D.J. Hare, S. Bohic, S.A. James, J.L. Billings, D.I. Finkelstein, P.A. Doble, K.L. Double, Comparative Study of Metal Quantification in Neurological Tissue Using Laser Ablation-Inductively Coupled Plasma-Mass Spectrometry Imaging and X-ray Fluorescence Microscopy, Analytical chemistry, 87 (2015) 6639-6645.
[64] R. Polishchuk, S. Lutsenko, Golgi in copper homeostasis: a view from the membrane trafficking field, Histochemistry and cell biology, 140 (2013) 285-295.
[65] K.A. Nugent, Coherent methods in the X-ray sciences, Advances in Physics, 59 (2010) 1-99.
[66] E. Kosior, S. Bohic, H. Suhonen, R. Ortega, G. Deves, A. Carmona, F. Marchi, J.F. Guillet, P. Cloetens, Combined use of hard X-ray phase contrast imaging and X-ray fluorescence microscopy for sub-cellular metal quantification, Journal of structural biology, 177 (2012) 239-247.
[67] N.P. Visanji, J.F. Collingwood, M.E. Finnegan, A. Tandon, E. House, L.N. Hazrati, Iron deficiency in parkinsonism: region-specific iron dysregulation in Parkinson's disease and multiple system atrophy, Journal of Parkinson's disease, 3 (2013) 523-537.

[68] S. Bohic, M. Cotte, M. Salome, B. Fayard, M. Kuehbacher, P. Cloetens, G. Martinez-Criado, R. Tucoulou, J. Susini, Biomedical applications of the ESRF synchrotron-based microspectroscopy platform, Journal of structural biology, 177 (2012) 248-258.
[69] A. Carmona, G. Deves, S. Roudeau, P. Cloetens, S. Bohic, R. Ortega, Manganese accumulates within golgi apparatus in dopaminergic cells as revealed by synchrotron X-ray fluorescence nanoimaging, ACS chemical neuroscience, 1 (2010) 194-203.
[70] D.B. Kell, Towards a unifying, systems biology understanding of large-scale cellular death and destruction caused by poorly liganded iron: Parkinson's, Huntington's, Alzheimer's, prions, bactericides, chemical toxicology and others as examples, Arch Toxicol, 84 (2010) 825-889.
[71] Y. Tao, Y. Wang, J.T. Rogers, F. Wang, Perturbed iron distribution in Alzheimer's disease serum, cerebrospinal fluid, and selected brain regions: a systematic review and meta-analysis, J Alzheimers Dis, 42 (2014) 679-690.
[72] A. White, Metals on our Mind, in: The Scientist, LabX Media Group, Ontario, Canada, 2014.
[73] B.A. Maher, I.A. Ahmed, V. Karloukovski, D.A. MacLaren, P.G. Foulds, D. Allsop, D.M. Mann, R. Torres-Jardon, L. Calderon-Garciduenas, Magnetite pollution nanoparticles in the human brain, Proceedings of the National Academy of Sciences of the United States of America, 113 (2016) 10797-10801.
[74] G. Plascencia-Villa, A. Ponce, J.F. Collingwood, M.J. Arellano-Jimenez, X. Zhu, J.T. Rogers, I. Betancourt, M. Jose-Yacaman, G. Perry, High-resolution analytical imaging and electron holography of magnetite particles in amyloid cores of Alzheimer's disease, Scientific reports, 6 (2016) 24873.
[75] J.F. Collingwood, A. Mikhaylova, M. Davidson, C. Batich, W.J. Streit, J. Terry, J. Dobson, In situ characterization and mapping of iron compounds in Alzheimer's disease tissue, J Alzheimers Dis, 7 (2005) 267-272.
[76] J.J. Gallagher, M.E. Finnegan, B. Grehan, J. Dobson, J.F. Collingwood, M.A. Lynch, Modest amyloid deposition is associated with iron dysregulation, microglial activation, and oxidative stress, J Alzheimers Dis, 28 (2012) 147-161.
[77] J. Everett, E. Cespedes, L.R. Shelford, C. Exley, J.F. Collingwood, J. Dobson, G. van der Laan, C.A. Jenkins, E. Arenholz, N.D. Telling, Evidence of redox-active iron formation following aggregation of ferrihydrite and the Alzheimer's disease peptide beta-amyloid, Inorg Chem, 53 (2014) 2803-2809.
[78] H. Wu, J.J. Yin, W.G. Wamer, M. Zeng, Y.M. Lo, Reactive oxygen species-related activities of nano-iron metal and nano-iron oxides, J Food Drug Anal, 22 (2014) 86-94.
[79] F. Ruiperez, J.I. Mujika, J.M. Ugalde, C. Exley, X. Lopez, Pro-oxidant activity of aluminum: promoting the Fenton reaction by reducing Fe(III) to Fe(II), Journal of inorganic biochemistry, 117 (2012) 118-123.
[80] P. Dusek, P.M. Roos, T. Litwin, S.A. Schneider, T.P. Flaten, J. Aaseth, The neurotoxicity of iron, copper and manganese in Parkinson's and Wilson's diseases, Journal of trace elements in medicine and biology : organ of the Society for Minerals and Trace Elements, 31 (2015) 193-203.
[81] A. Momose, J. Fukuda, Phase-contrast radiographs of nonstained rat cerebellar specimen, Medical physics, 22 (1995) 375-379.
[82] W. Britta, N. Jens-Friedrich, O. Christian, L.-K. Jannick, R. Michael, S. Tim, K. Sarah, X-ray nano-diffraction on cytoskeletal networks, New Journal of Physics, 14 (2012) 085013.
[83] J. Als-Nielsen, D. McMorrow, Elements of Modern X-ray Physics, 2nd ed., Wiley, 2011.
[84] D.H. Bilderback, P. Elleaume, E. Weckert, Review of third and next generation synchrotron light sources, Journal of Physics B: Atomic, Molecular and Optical Physics, 38 (2005) S773-S797.
[85] F. Adams, C. Barbante, Comprehensive Analytical Chemistry, Elsevier Science Ltd., 2015.
[86] Z. Qin, J.A. Caruso, B. Lai, A. Matusch, J.S. Becker, Trace metal imaging with high spatial resolution: applications in biomedicine, Metallomics : integrated biometal science, 3 (2011) 28-37.
[87] W. Chao, P. Fischer, T. Tyliszczak, S. Rekawa, E. Anderson, P. Naulleau, Real space soft x-ray imaging at 10 nm spatial resolution, Optics express, 20 (2012) 9777-9783.
[88] R. Siegele, N.R. Howell, P.D. Callaghan, Z. Pastuovic, Investigation of elemental changes in brain tissues following excitotoxic injury, Nuclear Instruments and Methods in Physics Research Section B: Beam Interactions with Materials and Atoms, 306 (2013) 125-128.

[89] W. Liu, G.E. Ice, J.Z. Tischler, A. Khounsary, C. Liu, L. Assoufid, A.T. Macrander, Short focal length Kirkpatrick-Baez mirrors for a hard x-ray nanoprobe, Review of Scientific Instruments, 76 (2005) 113701.
[90] I. Ordavo, S. Ihle, V. Arkadiev, O. Scharf, H. Soltau, A. Bjeoumikhov, S. Bjeoumikhova, G. Buzanich, R. Gubzhokov, A. Günther, R. Hartmann, P. Holl, N. Kimmel, M. Kühbacher, M. Lang, N. Langhoff, A. Liebel, M. Radtke, U. Reinholz, H. Riesemeier, G. Schaller, F. Schopper, L. Strüder, C. Thamm, R. Wedell, A new pnCCD-based color X-ray camera for fast spatial and energy-resolved measurements, Nuclear Instruments and Methods in Physics Research Section A: Accelerators, Spectrometers, Detectors and Associated Equipment, 654 (2011) 250-257.
[91] K. Janssens, W. De Nolf, G. Van der Snickt, F. Brenker, Recent trends in quantitative aspects of microscopic X-ray fluorescence analysis, Trends in Analytical Chemistry, 29 (2010) 464-478.
[92] B. Beckhoff, Reference-free X-ray spectrometry based on metrology using synchrotron radiation, Journal of Analytical Atomic Spectrometry, 23 (2008) 845-853.
[93] D. Devos, C. Moreau, J.C. Devedjian, J. Kluza, M. Petrault, C. Laloux, A. Jonneaux, G. Ryckewaert, G. Garcon, N. Rouaix, A. Duhamel, P. Jissendi, K. Dujardin, F. Auger, L. Ravasi, L. Hopes, G. Grolez, W. Firdaus, B. Sablonniere, I. Strubi-Vuillaume, N. Zahr, A. Destee, J.C. Corvol, D. Poltl, M. Leist, C. Rose, L. Defebvre, P. Marchetti, Z.I. Cabantchik, R. Bordet, Targeting chelatable iron as a therapeutic modality in Parkinson's disease, Antioxidants & redox signaling, 21 (2014) 195-210.
[94] M. Heidari, S.H. Gerami, B. Bassett, R.M. Graham, A.C. Chua, R. Aryal, M.J. House, J.F. Collingwood, C. Bettencourt, H. Houlden, M. Ryten, U.K.B.E. Consortium, J.K. Olynyk, D. Trinder, D.M. Johnstone, E.A. Milward, Pathological relationships involving iron and myelin may constitute a shared mechanism linking various rare and common brain diseases, Rare diseases, 4 (2016) e1198458.
[95] J. Sherman, The theoretical derivation of fluorescent X-ray intensities from mixtures, Spectrochimica Acta 7(1955) 283-306.
[96] A.D. Surowka, P. Wrobel, M.M. Marzec, D. Adamek, M. Szczerbowska-Boruchowska, Novel approaches for correction against the soft matrix effects in the quantitative elemental imaging of human substantia nigra tissue using synchrotron X-ray fluorescence, Spectrochimica Acta Part B: Atomic Spectroscopy, 123 (2016) 47-58.
[97] F. Billè, G. Kourousias, E. Luchinat, M. Kiskinova, A. Gianoncelli, X-ray fluorescence microscopy artefacts in elemental maps of topologically complex samples: Analytical observations, simulation and a map correction method, Spectrochimica Acta Part B: Atomic Spectroscopy, 122 (2016) 23-30.
[98] M.J. Hackett, P.G. Paterson, I.J. Pickering, G.N. George, Imaging Taurine in the Central Nervous System Using Chemically Specific X-ray Fluorescence Imaging at the Sulfur K-Edge, Analytical chemistry, 88 (2016) 10916-10924.
[99] M. Lo Conte, K.S. Carroll, The redox biochemistry of protein sulfenylation and sulfinylation, The Journal of biological chemistry, 288 (2013) 26480-26488.
[100] R. Ortega, Direct speciation analysis of inorganic elements in single cells using X-ray absorption spectroscopy, J. Anal. At. Spectrom., 26 (2011) 23-29.
[101] H. Yan, Y.S. Chu, Optimization of multilayer Laue lenses for a scanning X-ray microscope, Journal of synchrotron radiation, 20 (2013) 89-97.
[102] H. Eba, H. Ooyama, K. Sakurai, Combination of projection-based XRF, XAFS and XRD imagings for rapid spatial distribution analysis of a heterogeneous material, J. Anal. At. Spectrom., 31 (2016) 1105-1111.
[103] Y. Takahashi, Y. Nishino, R. Tsutsumi, H. Kubo, H. Furukawa, H. Mimura, S. Matsuyama, N. Zettsu, E. Matsubara, T. Ishikawa, K. Yamauchi, High-resolution diffraction microscopy using the plane-wave field of a nearly diffraction limited focused x-ray beam, Physical Review B, 80 (2009).
[104] S. Chen, J. Deng, D.J. Vine, Y.S.G. Nashed, Q. Jin, T. Peterka, C. Jacobsen, S. Vogt, Simultaneous x-ray nano-ptychographic and fluorescence microscopy at the bionanoprobe, in: B. Lai (Ed.) X-Ray Nanoimaging: Instruments and Methods II, Proceedings of SPIE, San Diego, 2015, pp. 95920I.
[105] G.D. Ciccotosto, S.A. James, M. Altissimo, D. Paterson, S. Vogt, B. Lai, M.D. de Jonge, D.L. Howard, A.I. Bush, R. Cappai, Quantitation and localization of intracellular redox active metals by X-

ray fluorescence microscopy in cortical neurons derived from APP and APLP2 knockout tissue, Metallomics : integrated biometal science, 6 (2014) 1894-1904.
[106] D. Bourassa, S.C. Gleber, S. Vogt, H. Yi, F. Will, H. Richter, C.H. Shin, C.J. Fahrni, 3D imaging of transition metals in the zebrafish embryo by X-ray fluorescence microtomography, Metallomics : integrated biometal science, 6 (2014) 1648-1655.
[107] M.D. de Jonge, C.G. Ryan, C.J. Jacobsen, X-ray nanoprobes and diffraction-limited storage rings: opportunities and challenges of fluorescence tomography of biological specimens, Journal of synchrotron radiation, 21 (2014) 1031-1047.
[108] L. Vincze, B. Vekemans, F.E. Brenker, G. Falkenberg, K. Rickers, A. Somogyi, M. Kersten, F. Adams, Three-dimensional trace element analysis by confocal X-ray microfluorescence imaging, Analytical chemistry, 76 (2004) 6786-6791.
[109] R. Dimper, H. Reichert, ESRF Upgrade Programme Phase II (2015-2022), Technical Design Study, in: ESRF Orange Book, European Synchrotron Radiation Facility, Grenoble, France, 2015.
[110] K. Sakurai, M. Mizusawa, X-ray diffraction imaging of anatase and rutile, Analytical chemistry, 82 (2010) 3519-3522.
[111] C.Y. Hemonnot, J. Reinhardt, O. Saldanha, J. Patommel, R. Graceffa, B. Weinhausen, M. Burghammer, C.G. Schroer, S. Koster, X-rays Reveal the Internal Structure of Keratin Bundles in Whole Cells, ACS nano, 10 (2016) 3553-3561.
[112] J.F. Collingwood, N.D. Telling, Iron oxides in the human brain, in: D. Faivre (Ed.) Iron Oxides: from nature to materials and from formation to applications, Wiley VCH, Weinheim, Germany, 2016.
[113] E.M. Duke, M. Razi, A. Weston, P. Guttmann, S. Werner, K. Henzler, G. Schneider, S.A. Tooze, L.M. Collinson, Imaging endosomes and autophagosomes in whole mammalian cells using correlative cryo-fluorescence and cryo-soft X-ray microscopy (cryo-CLXM), Ultramicroscopy, 143 (2014) 77-87.
[114] R. Carzaniga, M.-C. Domart, L.M. Collinson, E. Duke, Cryo-soft X-ray tomography: a journey into the world of the native-state cell, Protoplasma, 251 (2014) 449-458.
[115] M. Shariatgorji, P. Svenningsson, P.E. Andren, Mass Spectrometry Imaging, an Emerging Technology in Neuropsychopharmacology, Neuropsychopharmacology, 39 (2014) 34-49.
[116] E.L. Que, R. Bleher, F.E. Duncan, B.Y. Kong, S.C. Gleber, S. Vogt, S. Chen, S.A. Garwin, A.R. Bayer, V.P. Dravid, T.K. Woodruff, T.V. O'Halloran, Quantitative mapping of zinc fluxes in the mammalian egg reveals the origin of fertilization-induced zinc sparks, Nature chemistry, 7 (2015) 130-139.
[117] Y. Kashiv, J.R. Austin, 2nd, B. Lai, V. Rose, S. Vogt, M. El-Muayed, Imaging trace element distributions in single organelles and subcellular features, Scientific reports, 6 (2016) 21437.
[118] R. Mizutani, Y. Suzuki, X-ray microtomography in biology, Micron, 43 (2012) 104-115.
[119] L. Perrin, A. Carmona, S. Roudeau, R. Ortega, Evaluation of sample preparation methods for single cell quantitative elemental imaging using proton or synchrotron radiation focused beams, J. Anal. At. Spectrom., 30 (2015) 2525-2532.
[120] I. Yanagi, T. Ishida, K. Fujisaki, K. Takeda, Fabrication of 3-nm-thick Si3N4 membranes for solid-state nanopores using the poly-Si sacrificial layer process, Scientific reports, 5 (2015) 14656.
[121] E.A. Carter, B.S. Rayner, A.I. McLeod, L.E. Wu, C.P. Marshall, A. Levina, J.B. Aitken, P.K. Witting, B. Lai, Z. Cai, S. Vogt, Y.C. Lee, C.I. Chen, M.J. Tobin, H.H. Harris, P.A. Lay, Silicon nitride as a versatile growth substrate for microspectroscopic imaging and mapping of individual cells, Molecular bioSystems, 6 (2010) 1316-1322.
[122] E. Vergucht, T. Brans, F. Beunis, J. Garrevoet, S. Bauters, M. De Rijcke, D. Deruytter, C. Janssen, C. Riekel, M. Burghammer, L. Vincze, Methodological challenges of optical tweezers-based X-ray fluorescence imaging of biological model organisms at synchrotron facilities, Journal of synchrotron radiation, 22 (2015) 1096-1105.
[123] R. Van Noorden, 24 hours at the X-ray factory, Nature, 531 (2016) 564-567.
[124] F.J. Dyson, The Sun, The Genome, and The Internet: Tools of Scientific Revolution, New York Public Library, 2000.
[125] ESOF, General Meeting, in: 93rd Euroscience Open Forum, Manchester, 2016.
[126] R. Kitchin, Big Data, new epistemologies and paradigm shifts, Big Data & Society, 1 (2014) 1-12.

[127] J.F. Collingwood, F. Adams, X-ray microscopy for detection of metals in the brain, in: A. White (Ed.) Metals in the Brain: Measurement and Imaging, Springer, In press.